CHALMERS
UNIVERSITY OF TECHNOLOGY

UNIVERSITY OF GOTHENBURG

Numerical Analysis of Yield Curves Implied by Two-Factor Interest Rate Models

VERONIKA CHRONHOLM

Department of Mathematical Sciences
CHALMERS UNIVERSITY OF TECHNOLOGY
UNIVERSITY OF GOTHENBURG
Gothenburg, Sweden 2021

Thesis for the degree of Master of Science

Numerical Analysis of Yield Curves Implied by Two-Factor Interest Rate Models

VERONIKA CHRONHOLM

UNIVERSITY OF
GOTHENBURG

CHALMERS
UNIVERSITY OF TECHNOLOGY

Department of Mathematical Sciences
Chalmers University of Technology
University of Gothenburg
Gothenburg, Sweden 2021

Numerical Analysis of Yield Curves Implied by Two-Factor Interest Rate Models
Veronika Chronholm

Supervisor: Simone Calogero, Department of Mathematical Sciences
Examiner: Moritz Schauer, Department of Mathematical Sciences

Department of Mathematical Sciences
Chalmers University of Technology and University of Gothenburg
SE-412 96 Gothenburg
Telephone +46 (0)31- 772 10 00

Typeset in LaTeX
Gothenburg, Sweden 2021

Numerical Analysis of Yield Curves Implied by Two-Factor Interest Rate Models
Veronika Chronholm
Department of Mathematical Sciences
Chalmers University of Technology and University of Gothenburg

Abstract

We investigate the yield curves implied by coupon bonds in models where the market short rate is given by a two-factor stochastic model. Specifically, we investigate generalisations of the two-factor Vasicek, Cox-Ingersoll-Ross, and mixed models where the two Brownian motions that feature in each model are allowed to have nonzero constant correlation. We also study the two-factor Rendlemann-Bartter model with nonzero constant correlation. In all these models, we manage to recreate the four yield curve shapes commonly discussed in the literature; normal, steep, inverted, and flat. We also investigate how some of the interest rate model parameters affect the qualitative properties of the yield curves produced, and compare the yield curves obtained in the different models.

Acknowledgements

I would like to thank my supervisor Simone Calogero for his support and guidance throughout this project.

Veronika Chronholm, Gothenburg, May 2021

Contents

1

Introduction

The yield curve associated with a class of bonds tells us about the cost of borrowing and lending money by investing in those bonds. Historically, changes in the shape of the yield curve have happened before a significant economic change [6] [17], and it is thus of interest to be able to recreate the different shapes that the yield curve can take in a given numerical model. In the literature, the four different shapes are referred to as normal, inverted, steep, and flat or humped.

A yield curve plots the yield to maturity of bonds with varying maturities versus their maturity. The yield to maturity of a bond is the constant continuously compounded interest rate at which all future payments of the bond should be discounted to obtain its present value.

Institutions such as the Swedish National Debt Office and the United States Treasury issue coupon bonds as a way to finance public spending. It is thus of interest to specifically investigate coupon bond yield curves. A coupon bond is a financial contract which promises to pay some amount of money – the face value – at maturity, and some other amounts of money – the coupons – at other times between the present date and the time of maturity.

The aim of this thesis is to numerically investigate the coupon bond yield curves implied by two-factor interest rate models for the short rate. The short rate is defined as the continuously compounded, annualized interest rate at which money can be borrowed instantaneously and for an infinitesimally short time. The interest rate models considered are thus models in which the short rate is an affine function of two stochastic processes, which solve a system of two coupled stochastic differential equations. A benefit of two-factor models is that they allow for two different sources of uncertainty in the model, in the form of two Brownian motions, which can be either independent or correlated.

When modelling the interest rate, it might be of interest whether the chosen model can recreate the different qualitative behaviours of the yield curve. We thus attempt to recreate the main shapes that the yield curve can take in the different interest rate models that we study. We also investigate how allowing for correlation between the Brownian motions in the interest rate model affects the bond prices as well as the behaviour of the yield curve in the models.

The focus lies on the class of models known as two-factor affine interest rate models, namely the two-factor Vasicek, Cox-Ingersoll-Ross, and mixed models, where we allow for nonzero constant correlation between the two driving Brownian motions in each model. We also consider one non-affine model, the two-factor Rendlemann-Bartter model with constant correlation between the driving Brownian motions.

1.1 Outline

In chapter 2 we present some relevant background on financial mathematics. The concepts of zero coupon bonds and coupon bonds and the relationship between their prices are covered. We also discuss risk neutral pricing and the risk neutral pricing formula, and how to calculate the yield to maturity of a coupon bond.

Chapters 3, 4, and 5 are each divided into two parts; one theoretical and one that covers numerical methods. In the theoretical part of each chapter, theoretical concepts and properties are introduced, whereas relevant parts of the numerical methods and results are presented in the numerical methods part.

In chapter 3, we introduce the interest rate models that we study and discuss some of their theoretical properties, such as mean reversion, and existence and uniqueness of solutions for the Cox-Ingersoll-Ross and mixed models, where at least one factor in the model must remain posititive for all times t. We also discuss numerical methods for solving the stochastic differential equations of the models and thus generating paths of the interest rate. Specifically, we discuss the Euler-Maruyama scheme and some modifications of it for the Cox-Ingersoll-Ross model and the mixed model.

In chapter 4 we discuss the pricing of zero coupon bonds using the risk neutral pricing formula. We derive the partial differential equation for the price of a zero coupon bond, and discuss the case of affine yield models where the PDE can be separated into a system of ordinary differential equations. We also discuss how to use Monte-Carlo methods to numerically estimate the zero coupon bond price given by the risk neutral pricing formula, and compare the prices obtained using this method with the prices obtained by numerically solving the system of ODE that results from the pricing PDE, where possible.

In chapter 5, we discuss in more detail how to calculate the yield to maturity of a coupon bond, and how we choose the values of the coupons. In the numerical part of the chapter, our main numerical results are presented, in the form of numerically generated yield curves from the different interest rate models.

In chapter 6, we summarise the numerical results and present a brief discussion.

1.2 Method and Numerics

The main numerical methods employed in this thesis are Monte-Carlo and multi-level Monte-Carlo methods, in combination with Euler-Maruyama schemes to generate paths of the solutions to the stochastic differential equations that make up the interest rate models. To solve the system of ODE that the zero coupon bond pricing PDE separates into, the MatLab solver `ode45` has been used. All code is written in MatLab version 9.7 for Windows. Some sample code displaying a few of the different algorithms used can be found in the appendix, as can a few numerical convergence plots.

2

Background

2.1 Zero Coupon Bonds and Coupon Bonds

A zero coupon bond (ZCB) with face value K and maturity T is a contract that promises to pay the amount K at time T. Since holding a portfolio containing one share of a zero coupon bond with face value K and maturity T, is equivalent holding a portfolio with K shares of a zero coupon bond with face value 1 and maturity T, we can without loss of generality limit our discussion to bonds with face value 1.

A coupon bond with face value K, maturity T, and coupons $\{c_1, ..., c_N\}$ paid at times $\{t_1, ..., t_N\}$, where $0 < t_1 < ... < t_N = T$, is a contract which promises to pay the amount c_k at time t_k for k = 1,2,...,$(N-1)$ and the amount $(K + c_N)$ at maturity. Bonds with maturity 1 year or shorter do not pay any coupons, so a coupon bond with maturity 1 year simply pays the amount K at maturity, thus being equivalent to a zero coupon bond with maturity T and face value K.

Holding a coupon bond at time t gives the holder no right to coupons paid out before time t. As in the case of zero coupon bonds, it is enough to consider coupon bonds with face value 1.

For a time $t \in$ [0,T], holding a coupon bond which pays coupons as described above is equivalent to holding a portfolio consisting of shares of zero coupon bonds with face value 1 and with maturities $\{t_k, k : t_k > t\}$, where the number of shares of the coupon bond with maturity $t_N = T$ is $(1 + c_N)$ and the number of shares of the zero coupon bond with maturity t_k is c_k for all other k. In other words, if we let $k(t)$ be the smallest index such that $t_k > t$, then the value $B_c(t,T)$ of the coupon bond at time t is

$$B_c(t,T) = \sum_{i=k(t)}^{N-1} c_i B(t,t_i) + (1 + c_N)B(t,T) \tag{2.1}$$

where $B(t,t_k)$ is the price of the zero coupon bond with face value 1 and maturity t_k at time t. Thus, to calculate the price of a coupon bond at time t in a given market model, it is enough to be able to calculate the values at time t of zero coupon bonds with different maturities.

2.2 Risk Neutral Pricing

A sufficient condition for a market model to be arbitrage-free is the existence of a risk-neutral probability measure under which the discounted value of any portfolio in the market is a martingale.[16]

The risk-neutral pricing formula can be derived by considering a portfolio consisting of

one share of a given asset. The condition that the discounted value of the portfolio is a martingale, is then equivalent to requiring that the discounted asset price be a martingale in the risk-neutral probability measure. The discount factor $D(t)$ solves the differential equation $dD(t) = -R(t)D(t)dt$, where $R(t)$ is the interest rate, or short rate. The solution to this differential equation is

$$D(t) = \exp\Big(- \int_0^t R(s)ds\Big). \tag{2.2}$$

By requiring that the discounted price of a zero coupon bond at time t, $D(t)B(t,T)$ be a martingale in the risk-neutral probability measure we get

$$D(t)B(t,T) = \tilde{\mathbb{E}}[D(T)B(T,T) \mid \mathcal{F}(t)], \tag{2.3}$$

where $\mathcal{F}(t)$ is the filtration generated by the Brownian motion. Since we have restricted the discussion to zero coupon bonds with face value 1, by definition $B(T,T) = 1$. Further, $D(t)$ is $\mathcal{F}(t)$-measurable, meaning that we can divide both sides of the equation by $D(t)$ and bring it inside the expectation on the right hand side. Thus, we obtain

$$B(t,T) = \tilde{\mathbb{E}}\Big[\exp\Big(- \int_t^T R(s)ds\Big) \mid \mathcal{F}(t)\Big]. \tag{2.4}$$

In particular, the price at time zero of the zero coupon bond is

$$B(0,T) = \tilde{\mathbb{E}}\Big[\exp\Big(- \int_0^T R(s)ds\Big)\Big]. \tag{2.5}$$

In the above, the expectation is taken in the risk-neutral probability measure.

To go from the physical probability measure to the risk-neutral probability measure, one needs to determine the market price of risk. To do this, there needs to be a risky asset – such as a stock – in the market from which one can derive the so called market price of risk equations. Since we are working with a model where the dynamics of the short rate are specified instead, we don't have a risky asset given in the model from which we could get the market price of risk equations. To get around this problem, any interest rate model discussed in this thesis will be formulated directly in the risk-neutral probability measure.

2.3 Yield to Maturity and Yield Curves

In the case of a zero coupon bond with face value 1 and maturity T, the yield to maturity at a time $0 \leq t \leq T$ is the quantity $Y(t,T)$ for which it holds that

$$B(t,T) = e^{-Y(t,T)(T-t)}, \tag{2.6}$$

where $B(t,T)$ is the price of the zero coupon bond at time t.

The yield to maturity at time t of a coupon bond with maturity T is the quantity $Y_c(t,T)$ for which

$$B_c(t,T) = \sum_{i=k(t)}^{N-1} c_i e^{-Y_c(t,T)(t_i-t)} + (1+c_N)e^{-Y_c(t,T)(T-t)}. \tag{2.7}$$

Thus, if we know the price of the coupon bond at time t, we have an equation where the only unknown is $Y_c(t,T)$. Since $B_c(t,T)$ can be calculated from the prices of zero coupon bonds through equation (2.1), to compute the yield to maturity of a coupon bond in a given model, we simply need to be able to price zero coupon bonds and then solve equation (2.7) for the yield.

The yield to maturity at time zero, $Y_c(0,T)$ is given by

$$B_c(0,T) = \sum_{i=1}^{N-1} c_i e^{-Y_c(0,T)t_i} + (1+c_N)e^{-Y_c(0,T)T}. \tag{2.8}$$

If we measure time in years, and let both the maturity and all times at which a coupon is paid be integer numbers of years, equation (5.1) is simply a polynomial equation for $x = e^{-Y_c(0,T)}$, namely

$$\sum_{k=1}^{N-1} c_k x^k + (1+c_N)x^N - B_c(0,T) = 0. \tag{2.9}$$

This polynomial equation will be discussed in more detail in chapter 5.

3

Interest Rate Models

3.1 Theory

3.1.1 A Brief Note on the Existence and Uniqueness of Solutions to Multidimensional SDE

Consider a two-dimensional stochastic differential equation

$$d\mathbf{X}(t) = \mathbf{b}(\mathbf{X}(t), t)dt + \sigma(\mathbf{X}(t),t)d\mathbf{W}(t), \tag{3.1}$$

where σ is a 2×2 matrix, $\mathbf{b}$ is a two-dimensional vector, and $\mathbf{W}(t)$ is a two-dimensional Brownian motion. The SDE then has a unique strong global solution if the Lipschitz condition

$$|\mathbf{b}(\mathbf{x},t) - \mathbf{b}(\mathbf{y},t)| + |\sigma(\mathbf{x},t) - \sigma(\mathbf{y},t)| < K_T|\mathbf{x} - \mathbf{y}| \tag{3.2}$$

and the linear growth condition

$$|\mathbf{b}(\mathbf{x},t)| + |\sigma(\mathbf{x},t)| \leq K_T(1 + |\mathbf{x}|) \tag{3.3}$$

both hold for all t such that $0 \leq t \leq T$, and for all T, and where the constant K_T only depends on T [13]. In the above, the norm of the vector $\mathbf{b}$ is defined as $|\mathbf{b}| = \sqrt{b_1^2 + b_2^2}$, and the norm of the matrix σ is defined by $|\sigma|^2 = \mathrm{Tr}(\sigma\sigma^\top)$. We note that the conditions (3.2) and (3.3) are sufficient but not all necessary for the existence of a unique solution.

3.1.2 Introduction of Interest Rate Models

The studied interest rate models are two-factor interest rate models, where the market short rate is modelled by a stochastic process $R(t)$ that is a function of two factors $X_1(t)$ and $X_2(t)$ which solve some stochastic differential equations. Specifically, we study models of the form

$$R(t) = \delta_0 + \delta_1 X_1(t) + \delta_2 X_2(t) \tag{3.4a}$$
$$dX_1(t) = (\mu_1 - \lambda_{11}X_1(t) - \lambda_{12}X_2(t))dt + \sigma_1 X_1(t)^{\gamma_1} dW_1(t) \tag{3.4b}$$
$$dX_2(t) = (\mu_2 - \lambda_{21}X_1(t) - \lambda_{22}X_2(t))dt + \sigma_2 X_2(t)^{\gamma_2} dW_2(t). \tag{3.4c}$$

$W_1(t)$ and $W_2(t)$ are standard Brownian motions, i.e. continuous-time stochastic processes which have the following properties[13].

- $W_i(0) = 0$
- Independent increments: For $t > s$, $W_i(t) - W_i(s)$ is independent of the values taken up to time s, or of $W_i(u)$ for $0 \leq u < s$.
- Normal increments: $W_i(t) - W_i(s)$ is normally distributed with mean zero and variance $t - s$.
- Continuity of paths: The stochastic process $W_i(t)$ for $t \geq 0$ has almost surely continuous paths.

In this thesis, we consider the case where the Brownian motions $W_1(t)$ and $W_2(t)$ have constant correlation $\rho \in [-1,1]$, and thus $dW_1 dW_2 = \rho dt$. The parameters d_0, d_1, d_2, μ_1, μ_2, λ_{11}, λ_{12}, λ_{21}, λ_{22}, σ_1, and σ_2 are real constants, and γ_1, $\gamma_2 \in [0,1]$. Here, we study the two-factor Vasicek, Cox-Ingersoll-Ross (CIR), and mixed models, as well as the two-factor Rendleman-Bartter model.

The two factor Vasicek model

In the two-factor Vasicek model, $\gamma_1 = \gamma_2 = 0$ and the model is thus given by

$$R(t) = \delta_0 + \delta_1 X_1(t) + \delta_2 X_2(t) \tag{3.5a}$$
$$dX_1(t) = (\mu_1 - \lambda_{11} X_1(t) - \lambda_{12} X_2(t))dt + \sigma_1 dW_1(t) \tag{3.5b}$$
$$dX_2(t) = (\mu_2 - \lambda_{21} X_1(t) - \lambda_{22} X_2(t))dt + \sigma_2 dW_2(t). \tag{3.5c}$$

In the Vasicek model, both the factors $X_1(t)$ and $X_2(t)$ and the interest rate $R(t)$ are allowed to take both positive and negative values. The conditions (3.2) and (3.3) hold for all $\mathbf{x}, \mathbf{y}$ – and we note that the drift and diffusion are time imdependent – so the stochastic differential equations (3.5b)-(3.5c) have a unique strong solution.

The two factor CIR model

In the two-factor CIR model, $\gamma_1 = \gamma_2 = 0.5$ and the model is given by

$$R(t) = \delta_0 + \delta_1 X_1(t) + \delta_2 X_2(t) \tag{3.6a}$$
$$dX_1(t) = (\mu_1 - \lambda_{11} X_1(t) - \lambda_{12} X_2(t))dt + \sigma_1 \sqrt{X_1} dW_1(t) \tag{3.6b}$$
$$dX_2(t) = (\mu_2 - \lambda_{21} X_1(t) - \lambda_{22} X_2(t))dt + \sigma_2 \sqrt{X_2} dW_2(t). \tag{3.6c}$$

Since both factors $\{X_1(t)\}$ and $\{X_2(t)\}$ feature under a square root in the case of the CIR model, both factors must remain positive for the interest rate to remain real.

Furthermore, the Lipschitz condition (3.2) holds everywhere except at zero, where the derivative of the square root function is infinite. Thus, if we under some condition on the coefficients of the SDE can be sure that the process does not hit zero, we can say that the SDE has a unique strong solution.

In the case of the one-dimensional CIR model,

$$dX(t) = a(b - X(t))dt + \sigma \sqrt{X(t)} dW(t), \tag{3.7}$$

$X(t) > 0$ for all t almost surely when the so-called Feller condition $ab > \frac{\sigma^2}{2}$ holds, as long as the initial condition $X(0) > 0$, and where the constants a and b are assumed to be positive. Thus, under this condition, the one-dimensional CIR SDE has a unique strong solution.

In the case of the two-factor CIR model, we first consider the case when $\sigma_1 = \sigma_2 = 0$, when the system of SDE reduces to a system of ODE to get a necessary condition for positivity on the drift coefficients. We then get the system of ODE

$$\frac{dx_1(t)}{dt} = \mu_1 - \lambda_{11}x_1(t) - \lambda_{12}x_2(t) \tag{3.8a}$$

$$\frac{dx_2(t)}{dt} = \mu_2 - \lambda_{21}x_1(t) - \lambda_{22}x_2(t). \tag{3.8b}$$

For the function $x_1(t)$ to not become negative, we need its derivative to be nonnegative when $x_1(t) = 0$, and similarly the derivative of $x_2(t)$ must be nonnegative when $x_2(t) = 0$, meaning

$$\mu_1 - \lambda_{12}x_2 \geq 0 \tag{3.9}$$

$$\mu_2 - \lambda_{21}x_1 \geq 0 \tag{3.10}$$

This holds when $\mu_1 \geq 0$ and $\lambda_{12} \leq 0$, as long as $x_2(t) \geq 0$. Similarly, for $x_2(t)$ not to become negative, we require that $\mu_2 \geq 0$ and $\lambda_{21} \leq 0$.

Now, in the case where σ_1, $\sigma_2 \neq 0$, these conditions on the drift coefficients are not sufficient for the stochastic processes $X_1(t)$ and $X_2(t)$ to remain (strictly) positive. Similarly to in the one-factor CIR model, we also require a condition which involves the relationship between the drift parameters and the volatility parameters σ_1 and σ_2. A Feller condition for two-dimensional CIR processes is not widely studied in the literature, but a condition that can be applied to the two-factor CIR model with non-correlated Brownian motions is presented and proved in [7]. The condition is as follows. Consider a system of SDE of the form

$$d\mathbf{X}(t) = (\mu - \Lambda\mathbf{X}(t))dt + \Sigma \begin{pmatrix} \sqrt{\nu_1(\mathbf{X}(t))} & 0 \\ 0 & \sqrt{\nu_2(\mathbf{X}(t))} \end{pmatrix} d\mathbf{W}(t), \tag{3.11a}$$

where $\mathbf{W}(t)$ is a standard two-dimensional Brownian motion with zero correlation between the components, Σ and Λ are 2×2 constant matrices and μ is a constant vector. Furthermore,

$$\nu_i(\mathbf{x}) = a_i + \mathbf{b}_i \cdot \mathbf{x}. \tag{3.12}$$

The conditions for maintaining strict positivity of the two-dimensional process $\mathbf{X}(t)$ are then formulated as follows; for $i = 1,2$

$$\text{For all } \mathbf{x} \text{ such that } \nu_i(\mathbf{x}) = 0,\ \mathbf{b}_i^\top(\mu - \Lambda\mathbf{x}) > \frac{1}{2}\mathbf{b}_i^\top\Sigma\Sigma^\top\mathbf{b}_i \tag{3.13}$$

$$\text{For all } j, \text{ if } (\mathbf{b}_i^\top\Sigma)_j \neq 0,\ \text{then } \nu_i = \nu_j \tag{3.14}$$

In the case of the two-factor CIR model (3.6), $\mu = \begin{pmatrix}\mu_1\\ \mu_2\end{pmatrix}$, $\Lambda = \begin{pmatrix}\lambda_{11} & \lambda_{12}\\ \lambda_{21} & \lambda_{22}\end{pmatrix}$, $\Sigma = \begin{pmatrix}\sigma_1 & 0\\ 0 & \sigma_2\end{pmatrix}$, and $\nu_i(x) = x_i$, i.e. $a_1 = a_2 = 0$, $\mathbf{b}_1 = \begin{pmatrix}1\\0\end{pmatrix}$, and $\mathbf{b}_2 = \begin{pmatrix}0\\1\end{pmatrix}$. The condition (3.13) then becomes

$$\forall \mathbf{x} : x_1 = 0,\ \begin{pmatrix}1 & 0\end{pmatrix}\left[\begin{pmatrix}\mu_1\\ \mu_2\end{pmatrix} - \begin{pmatrix}\lambda_{11} & \lambda_{12}\\ \lambda_{21} & \lambda_{22}\end{pmatrix}\begin{pmatrix}0\\ x_2\end{pmatrix}\right] > \frac{1}{2}\begin{pmatrix}1 & 0\end{pmatrix}\begin{pmatrix}\sigma_1^2 & 0\\ 0 & \sigma_2^2\end{pmatrix}\begin{pmatrix}1\\ 0\end{pmatrix} \tag{3.15}$$

$$\forall \mathbf{x} : x_2 = 0,\ \begin{pmatrix}0 & 1\end{pmatrix}\left[\begin{pmatrix}\mu_1\\ \mu_2\end{pmatrix} - \begin{pmatrix}\lambda_{11} & \lambda_{12}\\ \lambda_{21} & \lambda_{22}\end{pmatrix}\begin{pmatrix}x_1\\ 0\end{pmatrix}\right] > \frac{1}{2}\begin{pmatrix}0 & 1\end{pmatrix}\begin{pmatrix}\sigma_1^2 & 0\\ 0 & \sigma_2^2\end{pmatrix}\begin{pmatrix}0\\ 1\end{pmatrix} \tag{3.16}$$

or equivalently

$$\mu_1 - \lambda_{12}x_2 > \frac{1}{2}\sigma_1^2 \tag{3.17a}$$

$$\mu_2 - \lambda_{21}x_1 > \frac{1}{2}\sigma_2^2. \tag{3.17b}$$

We note that these conditions are a stricter version of the conditions (3.9). Furthermore, if we as previously impose $\lambda_{12}, \lambda_{21} \leq 0$, we can simply require that $\mu_1 > \frac{1}{2}\sigma_1^2$ and $\mu_2 > \frac{1}{2}\sigma_2^2$. This is enough as long as x_1,$x_2 \geq 0$.

The condition (3.14) becomes trivial in the case of the two-factor CIR model (3.6), as we shall now see. For $i = 1$,

$$\begin{pmatrix}1 & 0\end{pmatrix}\begin{pmatrix}\sigma_1 & 0\\ 0 & \sigma_2\end{pmatrix} = \begin{pmatrix}\sigma_1 & 0\end{pmatrix}. \tag{3.18}$$

Only the first component is nonzero, meaning that it must hold that $\nu_1 = \nu_1$, which is clearly true. The same argument can be made for $i = 2$.

Thus a sufficient condition for the processes $X_1(t)$ and $X_2(t)$ to remain strictly positive for all t almost surely, is to require that the conditions (3.17) hold or alternatively, as we have chosen to do here, that $\lambda_{12}, \lambda_{21} \leq 0$ and $\mu_1 > \frac{1}{2}\sigma_1^2$ and $\mu_2 > \frac{1}{2}\sigma_2^2$. Under these conditions, the two-dimensional SDE (3.6) has a unique strong solution[7]. This is the case since the processes $X_1(t)$ and $X_2(t)$ never hit zero, which is the only point where the Lipschitz condition does not hold.

Finally, in the two-factor CIR model (3.6), the parameters δ_0, δ_1, and δ_2 are restricted to $\delta_0 \geq 0$, and δ_1,$\delta_2 > 0$, so that the interest rate remains positive.

The two factor mixed model

In the two-factor mixed model, one factor follows a CIR model and one factor follows a Vasicek model, so for example $\gamma_1 = 0.5$ and $\gamma_2 = 0$ so that the model is given by

$$R(t) = \delta_0 + \delta_1 X_1(t) + \delta_2 X_2(t) \tag{3.19a}$$

$$dX_1(t) = (\mu_1 - \lambda_{11}X_1(t) - \lambda_{12}X_2(t))dt + \sigma_1\sqrt{X_1(t)}dW_1(t) \tag{3.19b}$$

$$dX_2(t) = (\mu_2 - \lambda_{21}X_1(t) - \lambda_{22}X_2(t))dt + \sigma_2 dW_2(t). \tag{3.19c}$$

In the mixed model, one factor – here the factor $X_1(t)$ – must remain positive, whereas the other factor – here $X_2(t)$ – is allowed to become negative. To ensure that the factor $X_1(t)$ remains positive in theory, we for simplicity set the parameter $\lambda_{12} = 0$, and get the model

$$R(t) = \delta_0 + \delta_1 X_1(t) + \delta_2 X_2(t) \tag{3.20a}$$
$$dX_1(t) = (\mu_1 - \lambda_{11} X_1(t))dt + \sigma_1 \sqrt{X_1(t)} dW_1(t) \tag{3.20b}$$
$$dX_2(t) = (\mu_2 - \lambda_{21} X_1(t) - \lambda_{22} X_2(t))dt + \sigma_2 dW_2(t). \tag{3.20c}$$

We can then apply the Feller condition for the one factor CIR model to equation (3.20b) and note that $X_1(t) > 0$ for all t almost surely as long as $\mu_1 > \frac{\sigma_1^2}{2}$, and $X(0) > 0$. Under this condition, the SDE (3.20b) has a unique strong solution. Consequently, we can say that the system of SDE (3.20) has a unique strong solution.

The two factor Rendleman-Bartter model

Finally, we also consider the two-factor Rendleman-Bartter model, where $\gamma_1 = \gamma_2 = 1$, and the model is given by

$$R(t) = \delta_0 + \delta_1 X_1(t) + \delta_2 X_2(t) \tag{3.21a}$$
$$dX_1(t) = (\mu_1 - \lambda_{11} X_1(t) - \lambda_{12} X_2(t))dt + \sigma_1 X_1(t) dW_1(t) \tag{3.21b}$$
$$dX_2(t) = (\mu_2 - \lambda_{21} X_1(t) - \lambda_{22} X_2(t))dt + \sigma_2 X_2(t) dW_2(t). \tag{3.21c}$$

The drift and volatility fulfil the conditions (3.2) and (3.3), and thus a unique strong solution exists.

What is commonly referred to as the Rendleman-Bartter interest rate model, is the one-factor model

$$dR(t) = \theta R(t)dt + \gamma R(t)dW(t), \tag{3.22}$$

where the interest rate follows a geometric Brownian motion[11]. In this model the interest rate follows the same dynamics as a stock does in what is commonly called the Black-Scholes model. One problem with using the Black-Scholes model for interest rate dynamics, is that the process $R(t)$ is then not mean-reverting.

Here, we will mainly consider a modified version of the two-factor Rendleman-Bartter model which has the mean-reverting property, but we will also briefly consider the non-mean-reverting two-factor version of the model for comparison.

In the next section, we find the conditions on the coefficients in the general interest rate model (3.4) under which the interest rate is mean-reverting. In particular, under these conditions, the two-factor Rendleman-Bartter model discussed here is naturally also mean-reverting.

3.1.3 Mean Reversion of the Interest Rate

An important property of any interest rate model is that it replicates the mean-reverting property observed in interest rates in real markets. This means that in the limit as $t \to \infty$, the mean of the interest rate converges to a constant, finite value. We will now derive the conditions under which the two factor Vasicek model, CIR model, mixed model, and Rendleman-Bartter model are mean-reverting.

For the factors $X_1(t)$ and $X_2(t)$ to be mean reverting, the matrix of coefficients

$$\Lambda = \begin{pmatrix} \lambda_{11} & \lambda_{21} \\ \lambda_{12} & \lambda_{22} \end{pmatrix} \tag{3.23}$$

must have strictly positive eigenvalues[16]. We will now see why this is the case, and find the value that the expectation converges to. The stochastic differential equations (3.4b)-(3.4c) written in integral form are

$$X_1(t) = X_1(0) + \int_0^t (\mu_1 - \lambda_{11}X_1(s) - \lambda_{12}X_2(s))ds + \int_0^t \sigma_1 X_1(s)^{\gamma_1} dW_1(s) \tag{3.24a}$$

$$X_2(t) = X_2(0) + \int_0^t (\mu_2 - \lambda_{21}X_1(s) - \lambda_{22}X_2(s))ds + \int_0^t \sigma_2 X_2(s)^{\gamma_2} dW_2(s). \tag{3.24b}$$

Taking the expectation of both equations and using the linearity of expectation, we get

$$\mathbb{E}[X_1(t)] = X_1(0) + \mathbb{E}\left[\int_0^t (\mu_1 - \lambda_{11}X_1(s) - \lambda_{12}X_2(s))ds\right] + \mathbb{E}\left[\int_0^t \sigma_1 X_1(s)^{\gamma_1} dW_1(s)\right] \tag{3.25a}$$

$$\mathbb{E}[X_2(t)] = X_2(0) + \mathbb{E}\left[\int_0^t (\mu_2 - \lambda_{21}X_1(s) - \lambda_{22}X_2(s))ds\right] + \mathbb{E}\left[\int_0^t \sigma_2 X_2(s)^{\gamma_2} dW_2(s)\right]. \tag{3.25b}$$

We note that the expectation of the Itô integrals is zero, by the martingale property of the Itô integral, and then exchange the order of integration and expectation in the remaining terms to get

$$\mathbb{E}[X_1(t)] = X_1(0) + \int_0^t (\mu_1 - \lambda_{11}\mathbb{E}[X_1(s)] - \lambda_{12}\mathbb{E}[X_2(s)])ds \tag{3.26a}$$

$$\mathbb{E}[X_2(t)] = X_2(0) + \int_0^t (\mu_2 - \lambda_{21}\mathbb{E}[X_1(s)] - \lambda_{22}\mathbb{E}[X_2(s)])ds, \tag{3.26b}$$

having also used the linearity of expectation again. Noting that the expectations of $X_1(t)$ and $X_2(t)$ will both be deterministic functions of t, which we can label $\mathbb{E}[X_1(t)] = v_1(t)$ and $\mathbb{E}[X_2(t)] = v_2(t)$ we get the coupled ordinary differential equations

$$\frac{d}{dt}v_1(t) = \mu_1 - \lambda_{11}v_1(t) - \lambda_{12}v_2(t) \tag{3.27a}$$

$$\frac{d}{dt}v_2(t) = \mu_2 - \lambda_{21}v_1(t) - \lambda_{22}v_2(t) \tag{3.27b}$$

or in vector form

$$\frac{d}{dt}v(t) + \Lambda v(t) = \mu \tag{3.28}$$

where $\mathbf{v}(t) = \begin{pmatrix} v_1(t) \\ v_2(t) \end{pmatrix}$, $\mu = \begin{pmatrix} \mu_1 \\ \mu_2 \end{pmatrix}$, and Λ is the matrix of coefficients defined in equation (3.23). The solution to (3.28) is given by the general solution to the homogeneous problem,

plus a particular solution. Since the right hand side is a constant vector, a particular solution that is also a constant vector can easily be found using the method of undetermined coefficients. Using the ansatz $\mathbf{v}^p(t) = \begin{pmatrix} a_1 \\ a_2 \end{pmatrix}$, where a_1 and a_2 are real constants, and noting that clearly the time derivative of a constant vector is zero, we find

$$\Lambda \mathbf{v}^p = \mu \implies \mathbf{v}^p = \Lambda^{-1}\mu, \tag{3.29}$$

where Λ^{-1} denotes the matrix inverse of Λ.

The general homogeneous solution is found by finding the eigenvalues and eigenvectors of the matrix Λ. Denoting the eigenvalues by r_1 and r_2, and the eigenvectors by $\boldsymbol{\xi_1}$ and $\boldsymbol{\xi_2}$, the general homogeneous solution is given by

$$\mathbf{v}^h(t) = c_1 \boldsymbol{\xi_1} e^{-r_1 t} + c_2 \boldsymbol{\xi_2} e^{-r_2 t}, \tag{3.30}$$

where c_1 and c_2 are real constants determined by the initial condition. Thus, the general solution to (3.28) is given by

$$\mathbf{v}(t) = \Lambda^{-1}\mu + c_1 \boldsymbol{\xi_1} e^{-r_1 t} + c_2 \boldsymbol{\xi_2} e^{-r_2 t}. \tag{3.31}$$

Considering the limit as $t \to \infty$, we see that as long as r_1 and r_2 are real, the limit exists if and only if r_1 and r_2 are strictly positive, and in that case

$$\lim_{t\to\infty} \mathbf{v}(t) = \Lambda^{-1}\mu. \tag{3.32}$$

We recall that r_1 and r_2 are the eigenvalues of Λ, and thus we have shown that the general interest rate model (3.4) is mean reverting if and only if the matrix Λ has strictly positive eigenvalues. In that case,

$$\lim_{t\to\infty} \mathbb{E}[\mathbf{X}(\mathbf{t})] = \Lambda^{-1}\mu, \tag{3.33}$$

where $\mathbf{X}(\mathbf{t}) = \begin{pmatrix} X_1(t) \\ X_2(t) \end{pmatrix}$. We note also that the inverse of the matrix Λ always exists if the matrix has positive eigenvalues. Since the relationship between the short rate $R(t)$ and the two factors $X_1(t)$ and $X_2(t)$ is given by (3.4a), we have

$$\lim_{t\to\infty} \mathbb{E}[R(t)] = \delta_0 + \delta^\top \Lambda^{-1}\mu, \tag{3.34}$$

where $\delta^\top = \begin{pmatrix} \delta_1 & \delta_2 \end{pmatrix}$. It is thus important that the parameters of the interest rate model are chosen such that the quantity on the right hand side of (3.34) is of the order of magnitude of an interest rate.

We note that in the case of the mixed model, where we have restricted to the case where $\lambda_{12} = 0$, the matrix Λ is triangular, and its eigenvalues are thus given by its diagonal entries.

Thus the requirement that Λ have positive eigenvalues is in the case of the mixed model equivalent to requiring that $\lambda_{11}, \lambda_{22} > 0$.

In the case of the Rendleman-Bartter model, where we want to investigate both the mean-reverting and non-mean-reverting versions of the model, for the latter the matrix of coefficients Λ should be chosen to have negative eigenvalues.

3.1.4 Meaning of Parameter Values

As we have just seen, the quantity $\Lambda^{-1}\mu$ features in the limit as $t \to \infty$ of the expectation of the interest rate. If we let the parameters δ_1 and δ_2 be such that the interest rate is the weighted average of the two factors $X_1(t)$ and $X_2(t)$, this means that for the mean interest rate to converge to a sensible value, the quantity $\Lambda^{-1}\mu$ should be of the order of magnitude of an interest rate, as should the parameter δ_0. By the order of magnitude of an interest rate, we here mean roughly between -0.1 and 0.1, or between -10 percent and $+10$ percent.

Naturally, the initial values of the factors X_1 and X_2, $X_1(0)$, and $X_2(0)$ should also be of the order of magnitude of an interest rate.

Finally, we should discuss the sensible range of values for the parameters σ_1 and σ_2, which determine the scale of the volatility of the interest rate. We choose σ_1 and σ_2 to be positive, and between 1 and 10 percent.

3.2 Numerical Methods

3.2.1 Euler-Maruyama Finite Difference Schemes

To simulate paths of the interest rate $R(t)$, we numerically solve the SDE (3.4). This is easily done using an Euler-Maruyama scheme, which for the general interest rate model (3.4) is given by

$$\begin{aligned} X_1(t_{n+1}) &= X_1(t_n) + (\mu_1 - \lambda_{11}X_1(t_n) - \lambda_{12}X_2(t_n)(t_{n+1} - t_n) \\ &\quad + \sigma_1 X_1(t_n)^{\gamma_1}(W_1(t_{n+1}) - W_1(t_n)) \end{aligned} \tag{3.35a}$$

$$\begin{aligned} X_2(t_{n+1}) &= X_2(t_n) + (\mu_1 - \lambda_{21}X_1(t_n) - \lambda_{22}X_2(t_n))(t_{n+1} - t_n) \\ &\quad + \sigma_2 X_2(t_n)^{\gamma_2}(W_2(t_{n+1}) - W_2(t_n)). \end{aligned} \tag{3.35b}$$

In the case of the two factor Vasicek model and the two factor Rendleman-Bartter model, we simply use the Euler-Maruyama scheme (3.35) as it is. However, for the two factor CIR and mixed models some modifications need to be made.

The Brownian increments $W_i(t_{n+1}) - W_i(t_n)$ are normally distributed with mean zero and variance $t_{n+1} - t_n$, and are thus simulated by generating normally distributed random numbers.

We have established conditions on the model parameters under which the factors that appear under square roots remain positive in the CIR and mixed models. However, even under these conditions the discretised versions of the processes appearing in the Euler-Maruyama scheme have a nonzero probability of becoming negative. If this happens in a numerical simulation, the next step in the scheme cannot be computed, as it would involve taking the square root of a negative number, yielding a complex number. This frequently happens in numerical simulations of the two-factor CIR model using the non-modified Euler-Maruyama scheme, especially for larger time steps.

A simple way to avoid this problem would be to keep generating each step in the scheme with new random numbers until it yields a positive result, but doing this gives an algorithm

that takes a random amount of time to run. Instead, we make modifications to the Euler-Maruyama scheme to ensure the positivity of the factors. Many different ways to do this exist, but here we will focus on two different modifications of the scheme.

The first is the so-called symmetrised Euler-Maruyama scheme, where one simply takes the absolute value of the regular scheme to obtain

$$\begin{aligned} X_1(t_{n+1}) = |X_1(t_n) &+ (\mu_1 - \lambda_{11}X_1(t_n) - \lambda_{12}X_2(t_n)(t_{n+1} - t_n) \\ &+ \sigma_1\sqrt{X_1(t_n)}(W_1(t_{n+1}) - W_1(t_n))| \end{aligned} \tag{3.36a}$$

$$\begin{aligned} X_2(t_{n+1}) = |X_2(t_n) &+ (\mu_1 - \lambda_{21}X_1(t_n) - \lambda_{22}X_2(t_n))(t_{n+1} - t_n) \\ &+ \sigma_2\sqrt{X_2(t_n)}(W_2(t_{n+1}) - W_2(t_n))| \end{aligned} \tag{3.36b}$$

for the CIR model. For the mixed model, we will use a half-symmetrised scheme of the form

$$\begin{aligned} X_1(t_{n+1}) = |X_1(t_n) &+ (\mu_1 - \lambda_{11}X_1(t_n))(t_{n+1} - t_n) \\ &+ \sigma_1\sqrt{X_1(t_n)}(W_1(t_{n+1}) - W_1(t_n))| \end{aligned} \tag{3.37a}$$

$$\begin{aligned} X_2(t_{n+1}) = X_2(t_n) &+ (\mu_1 - \lambda_{21}X_1(t_n) - \lambda_{22}X_2(t_n))(t_{n+1} - t_n) \\ &+ \sigma_2(W_2(t_{n+1}) - W_2(t_n)). \end{aligned} \tag{3.37b}$$

Note that in the scheme for the mixed model above, we have set the parameter value λ_{12} to zero, as discussed previously.

Strong convergence results for the symmetrised Euler-Maruyama scheme in the one dimensional case can be found in [2], for values of the exponent γ between 0.5 and 1.

A benefit of the symmetrised scheme is that the approximation processes preserve the positivity of the factors, which not all schemes do.

The second scheme that we will consider is the scheme suggested in [14]. This scheme also preserves positivity in the approximation process. The main idea of the scheme is to sample random numbers from a different distribution, rather than from a normal distribution, thus creating a Markov chain approximation scheme which is guaranteed to remain positive. Weak convergence of the whole path of the approximation process to that of the weak solution to the SDE is shown in [14] in the general multidimensional case.

In the general case, the scheme is formulated as follows. Consider the d-dimensional SDE

$$d\mathbf{X}(t) = \mathbf{b}(t, \mathbf{X}(t))dt + \sigma(t, \mathbf{X}(t))d\mathbf{W}(t) \tag{3.38}$$

where the drift $\mathbf{b} : \mathbb{R}_+ \times \mathbb{R}^d \to \mathbb{R}^d$ and the diffusion $\sigma : \mathbb{R}_+ \times \mathbb{R}^d \to \mathbb{R}^d \otimes \mathbb{R}^d$ are both continuous functions, and $\mathbb{R}^d \otimes \mathbb{R}^d$ is the space of $d \times d$ matrices. We also require that the SDE has a unique weak solution for each initial condition $\mathbf{X}(0) \in E := \mathbb{R}_+^m \times \mathbb{R}^{d-m}$, such that $\mathbf{X}(t) \in E$ for all $t \geq 0$. The approximating scheme with constant time step $\frac{1}{n}$ is then given by

$$\mathbf{X}(k+1) = \mathbf{X}(k) + \frac{1}{n}\mathbf{b}\Big(\frac{k}{n}, \mathbf{X}(k)\Big) + \frac{1}{\sqrt{n}}\tilde{\sigma}\Big(\frac{k}{n}, \mathbf{X}(k)\Big)(\varepsilon_k - \alpha) \tag{3.39}$$

where the continuous function $\tilde{\sigma} : \mathbb{R}_+ \times E \to \mathbb{R}^d \otimes \mathbb{R}^d$ is defined by the relation $\sigma\sigma^\top = \tilde{\sigma}\Sigma\tilde{\sigma}^\top$, and where Σ is a symmetric semi-definite positive $d \times d$ matrix. Further, ε_k for $k = 0,1,2...$

are independent identically distributed random vectors with mean vector α and covariance matrix Σ, such that $\mathbb{P}(\tilde{\sigma}(t,\mathbf{x})\varepsilon_k \in E\ \forall(t,\mathbf{x}) \in \mathbb{R}_+ \times E) = 1$.

Furthermore, the following condition on the choice of mean vector and smallest allowed value of n, where $\frac{1}{n}$ is the time step must hold;

$$\inf_{(t,\mathbf{x})\in\mathbb{R}_+\times E}\left(\mathbf{x} + \frac{1}{n}\mathbf{b}(t,\mathbf{x}) - \frac{1}{\sqrt{n}}\tilde{\sigma}(t,\mathbf{x})\alpha\right) \in E\ \forall n \geq n_0. \tag{3.40}$$

We note that both in the two factor CIR model and the mixed model, drift and diffusion functions are continuous. We have also previously noted that the SDE in both models have unique strong solutions, which implies that they also have unique weak solutions[13].

For the CIR model, we have

$$\tilde{\sigma} = \begin{pmatrix} \sigma_1\sqrt{X_1(t)} & 0 \\ 0 & \sigma_2\sqrt{X_2(t)} \end{pmatrix}, \tag{3.41}$$

$$\mathbf{b} = \begin{pmatrix} \mu_1 - \lambda_{11}X_1 - \lambda_{12}X_2 \\ \mu_2 - \lambda_{21}X_1 - \lambda_{22}X_2 \end{pmatrix}, \tag{3.42}$$

and

$$\Sigma = \begin{pmatrix} 1 & \rho \\ \rho & 1 \end{pmatrix}, \tag{3.43}$$

since the correlation between the two Brownian motions in the model is ρ.

Thus, the approximation scheme for the two factor CIR model is given by

$$X_1(k+1) = X_1(k) + \frac{1}{n}(\mu_1 - \lambda_{11}X_1(k) - \lambda_{12}X_2(k)) + \frac{1}{\sqrt{n}}\sigma_1\sqrt{X_1(k)}(\varepsilon_{k,1} - \alpha_1) \tag{3.44a}$$

$$X_2(k+1) = X_2(k) + \frac{1}{n}(\mu_2 - \lambda_{21}X_1(k) - \lambda_{22}X_2(k)) + \frac{1}{\sqrt{n}}\sigma_2\sqrt{X_2(k)}(\varepsilon_{k,2} - \alpha_2) \tag{3.44b}$$

The two factor CIR model is discussed specifically in [14], and it is found that the condition (3.40) holds when $n_0 > \max(\lambda_{11}, \lambda_{22})$, and $0 < \alpha_i < 2\sqrt{\mu_i(1 - \frac{\lambda_{ii}}{n_0})}$ for $i = 1,2$, and the random vector ε has non-negative components. Further, it is possible to construct a non-negative random vector ε with mean vector α and covariance matrix Σ if and only if $-\rho \leq \alpha_1\alpha_2$. Thus it is possible to choose n_0 and α such that the condition (3.40) holds as long as $-\rho < 4\sqrt{\mu_1\mu_2}$.

Moving on to the mixed model, we have

$$\tilde{\sigma} = \begin{pmatrix} \sigma_1\sqrt{X_1(t)} & 0 \\ 0 & \sigma_2 \end{pmatrix}, \tag{3.45}$$

$$\mathbf{b} = \begin{pmatrix} \mu_1 - \lambda_{11}X_1 \\ \mu_2 - \lambda_{21}X_1 - \lambda_{22}X_2 \end{pmatrix}, \tag{3.46}$$

and the same correlation matrix Σ as in the CIR model.

Thus, the approximation scheme for the two factor mixed model is

$$X_1(k+1) = X_1(k) + \frac{1}{n}(\mu_1 - \lambda_{11}X_1(k)) + \frac{1}{\sqrt{n}}\sigma_1\sqrt{X_1(k)}(\varepsilon_{k,1} - \alpha_1) \tag{3.47a}$$

$$X_2(k+1) = X_2(k) + \frac{1}{n}(\mu_2 - \lambda_{21}X_1(k) - \lambda_{22}X_2(k)) + \frac{1}{\sqrt{n}}\sigma_2(\varepsilon_{k,2} - \alpha_2). \tag{3.47b}$$

The condition (3.40) becomes

$$\inf_{(x_1,x_2)\in\mathbb{R}_+\times\mathbb{R}} \left(\mathbf{x} + \frac{1}{n}\mathbf{b}(t,\mathbf{x}) - \frac{1}{\sqrt{n}}\tilde{\sigma}(t,\mathbf{x})\alpha\right) \in \mathbb{R}_+ \times \mathbb{R} \ \forall n \geq n_0, \tag{3.48}$$

and we note that it is enough to consider the condition on the first component, since clearly the second component remains real if the first component remains positive. Thus we have the condition

$$\inf_{x_1\in\mathbb{R}_+} \left(x_1 + \frac{1}{n}(\mu_1 - \lambda_{11}x_1) - \frac{1}{\sqrt{n}}\sigma_1\sqrt{x_1}\alpha_1\right), \tag{3.49}$$

which holds when we choose $n_0 > \lambda_{11}$ and $0 < \alpha_1 \leq \frac{2}{\sigma_1}\sqrt{\mu_1(\frac{\lambda_{11}}{n_0})}$, as discussed in [14].

Clearly we need to make a specific choice for the distribution of the random vector ε to implement the schemes (3.44) and (3.44). In [14], the suggestion of using a Bernoulli-type random vector is put forward, and it is noted that this is a good choice since it is computationally cheap to generate Bernoulli distributed random numbers. We shall make the same choice here, and outline the details below. Specifically, the distribution of ε is chosen so that for $i = 1,2$

$$\frac{\alpha_i\varepsilon_i}{\alpha_i^2+1} \sim \text{Bern}\left(\frac{\alpha_i^2}{1+\alpha_i^2}\right), \tag{3.50}$$

where ε_i are the components of the random vector ε, and α_i are the components of its mean. Equivalently,

$$\mathbb{P}(\varepsilon_i = 0) = \frac{1}{1+\alpha_i^2} \text{ and } \mathbb{P}\left(\varepsilon_i = \frac{\alpha_i^2+1}{\alpha_i}\right) = \frac{\alpha_i^2}{1+\alpha_i^2}. \tag{3.51}$$

We note that it must hold that the quantity $\frac{\alpha_i^2}{1+\alpha_i^2} \in (0,1)$, as it is a probability.

To generate the random vector ε, we generate each of its components by first generating a uniformly distributed random number r_i in the interval (0,1), and then setting $\varepsilon_i = \frac{\alpha_i^2+1}{\alpha_i}$ if $r_i < \frac{\alpha_i^2}{1+\alpha_i^2}$ and $\varepsilon_i = 0$ otherwise.

3.2.2 Modelling SDE with Correlated Brownian Motions

In all the interest rate models that we consider, the correlation ρ between the two driving Brownian motions is potentially nonzero. To numerically simulate the paths of the interest

rate factors X_1 and X_2, as well as the interest rate itself, we must thus be able to numerically generate random numbers with constant correlation $\rho \in (-1,1)$.

Given two independent Brownian motions $W_1(t)$ and $W_2(t)$, the process $W^\rho(t)$ given by

$$W^\rho(t) = \rho W_1(t) + \sqrt{1-\rho^2} W_2(t) \tag{3.52}$$

is also a Brownian motion, and the correlation between $W_1(t)$ and $W^\rho(t)$ is equal to ρ[5]. Or equivalently, given a two-dimensional Brownian motion $\mathbf{B}(t)$ with independent components, the two-dimensional Brownian motion $\mathbf{W}(t)$ given by

$$\mathbf{W}(t) = \begin{pmatrix} 1 & 0 \\ \rho & \sqrt{1-\rho^2} \end{pmatrix} \mathbf{B}(t) \tag{3.53}$$

has the correlation matrix

$$\begin{pmatrix} 1 & \rho \\ \rho & 1 \end{pmatrix}. \tag{3.54}$$

In the regular Euler-Maruyama schemes for the Vasicek model and the Rendleman-Bartter model, and in the symmetrised schemes for the CIR and mixed models, we can simply multiply each independent two dimensional Brownian motion increment by the matrix

$$\begin{pmatrix} 1 & 0 \\ \rho & \sqrt{1-\rho^2} \end{pmatrix} \tag{3.55}$$

to generate the correlated Brownian motion increments, since we are using normally distributed random numbers with mean zero to model the Brownian increments.

In the weak scheme taken from [14], we instead use Bernoulli-type random numbers with nonzero mean, and then subtract the mean value. In this case, some more care is required. Given a random vector ε with independent components ε_1 and ε_2 that follow the distribution (3.51), with $\alpha_1 = \alpha_2 = a$, the random vector $\tilde{\varepsilon}$ defined by

$$\tilde{\varepsilon} = \begin{pmatrix} 1 & 0 \\ \rho & \sqrt{1-\rho^2} \end{pmatrix} \varepsilon \tag{3.56}$$

has correlation matrix

$$\begin{pmatrix} 1 & \rho \\ \rho & 1 \end{pmatrix} \tag{3.57}$$

as required, and mean vector

$$\tilde{\alpha} = \begin{pmatrix} a \\ a(\rho + \sqrt{1-\rho^2}) \end{pmatrix}. \tag{3.58}$$

Thus, in the schemes (3.44) and (3.47) the mean vector $\tilde{\alpha}$ should be subtracted, rather than the mean vector α of the original random vector ε with independent components. We note that when $\rho = 0$ the two coincide.

3.2.3 Numerical correlation of the factors X1 and X2

When the matrix of coefficients Λ is diagonal, the only source of correlation between two factors $X_1(t)$ and $X_2(t)$ in the general interest rate model should be the correlation ρ between the two Brownian motions. We now compare the numerical correlation between the factors $X_1(t)$ and $X_2(t)$ to the theoretical correlation ρ between the driving Brownian motions. We make comparisons in all the four studied interest rate models, and using the different discretisation schemes that have been discussed.

For the numerical correlation, we generate 10,000 paths each of X_1 and X_2, and then look at the numerical correlation between $X_1(T)$ and $X_2(T)$, where T is the endpoint of the simulated paths. It can be seen in table 3.1 that the numerical correlation agrees well with the correlation ρ between the Brownian motions in all cases.

Vasicek Euler-Maruyama Scheme							
ρ	-1	-0.9	-0.5	0	0.5	0.9	1
Num. Correlation	-0.9978	-0.8977	-0.5047	-0.0048	0.5029	0.8989	1.0
CIR Weak Scheme							
ρ	-1	-0.9	-0.5	0	0.5	0.9	1
Num. Correlation	-0,9743	-0.8786	-0.4888	0.0080	0.4960	0.8988	1.0
CIR Symmetrised Scheme							
ρ	-1	-0.9	-0.5	0	0.5	0.9	1
Num. Correlation	-0,8793	-0.7995	-0.4643	0.0124	0.4801	0.8943	1.0
Mixed Model Weak Scheme							
ρ	-1	-0.9	-0.5	0	0.5	0.9	1
Num. Correlation	-0,9933	-0.8933	-0.5022	$4 \cdot 10^{-4}$	0.4994	0.8960	0.9934
Mixed Model Symmetrised Scheme							
ρ	-1	-0.9	-0.5	0	0.5	0.9	1
Num. Correlation	-0,9727	-0.8757	-0.4818	0.0074	0.4854	0.8742	0.9731
Rendleman-Bartter Euler-Maruyama Scheme							
ρ	-1	-0.9	-0.5	0	0.5	0.9	1
Num. Correlation	-0,9941	-0.8924	-0.5028	0.0129	0.4854	0.8998	1.00

Table 3.1: Table showing comparisons between the numerical correlation between the factors $X_1(t)$ and $X_2(t)$ and the correlation ρ between the two Brownian motions in each model. The correlation agrees well for all interest rate models, and for all different numerical schemes studied.

4

Zero Coupon Bond Pricing

4.1 Theory

4.1.1 The Pricing PDE

Here, we derive the pricing PDE for a zero coupon bond in a two-factor interest rate model of the form studied in this thesis.

Recall the general interest rate model (3.4) that was introduced in chapter 3,

$$R(t) = \delta_0 + \delta_1 X_1(t) + \delta_2 X_2(t) \tag{4.1a}$$
$$dX_1(t) = (\mu_1 - \lambda_{11} X_1(t) - \lambda_{12} X_2(t))dt + \sigma_1 (X_1(t))^{\gamma_1} dW_1(t) \tag{4.1b}$$
$$dX_2(t) = (\mu_2 - \lambda_{21} X_1(t) - \lambda_{22} X_2(t))dt + \sigma_2 (X_2(t))^{\gamma_2} dW_2(t), \tag{4.1c}$$

and the risk-neutral pricing formula for the zero coupon bond with maturity T

$$B(t,T) = \tilde{\mathbb{E}}\Big[\exp\Big(-\int_t^T R(s)ds\Big) \mid \mathcal{F}(t)\Big]. \tag{4.2}$$

Recall further that the risk-neutral pricing formula was derived by requiring that the discounted ZCB price be a martingale in the risk-neutral probability measure, and that the interest rate model is formulated in the risk neutral probability measure.

Since the short rate $R(t)$ is a function of the factors $X_1(t)$ and $X_2(t)$, which solve the stochastic differential equations (4.1b)-(4.1c) and are thus Markov processes, there must exist some function $f(t,x_1,x_2)$ such that

$$B(t,T) = f(t,X_1,X_2). \tag{4.3}$$

Since the discounted bond price is a martingale in the risk neutral probability measure, the differential $d(D(t)B(t,T))$ must have dt-term zero. Here, as previously, $D(t)$ is the discounting factor, which is given by

$$D(t) = \exp\Big(-\int_0^t R(s)ds\Big), \tag{4.4}$$

and satisfies the differential equation $dD(t) = -R(t)D(t)dt$.

Computing the differential $d(D(t)B(t,T))$, we first use (4.3), Itô's product rule, and the differential equation for the discounting factor. Itô's formula then allows us to expand $df(t, X_1(t), X_2(t))$ in terms of the differentials dX_1 and dX_2.

$$d(D(t)B(t,T)) = d(D(t)f(t, X_1(t), X_2(t)) = \tag{4.5}$$
$$= -R(t)D(t)f(t, X_1(t), X_2(t))dt + D(t)df(t, X_1(t), X_2(t)) \tag{4.6}$$
$$= D\Big[- Rfdt + f_t dt + f_{x_1} dX_1 + f_{x_2} dX_2 + \frac{1}{2} f_{x_1 x_1} dX_1 dX_1 + \tag{4.7}$$
$$+ f_{x_1 x_2} dX_1 dX_2 + \frac{1}{2} f_{x_2 x_2} dX_2 dX_2 \Big] \tag{4.8}$$

Calculating the second order differentials using (4.1), and $dW_i dt = 0$, $dW_i dW_i = dt$, for $i = 1{,}2$ along with $dW_1 dW_2 = \rho dt$, we get

$$dX_1 dX_1 = \sigma_1^2 X_1(t)^{2\gamma_1} dt \tag{4.9}$$
$$dX_2 dX_2 = \sigma_2^2 X_2(t)^{2\gamma_2} dt \tag{4.10}$$
$$dX_1 dX_2 = \sigma_1 \sigma_2 X_1(t)^{\gamma_1} X_2(t)^{\gamma_2} dW_1(t) dW_2(t) = \rho \sigma_1 \sigma_2 X_1(t)^{\gamma_1} X_2(t)^{\gamma_2} dt. \tag{4.11}$$

Using these expressions for the differentials $dX_1 dX_1$, $dX_2 dX_2$ and $dX_1 dX_2$, and the expressions for dX_1 and dX_2 given by the SDE (4.1), in (4.5), we get

$$d(D(t)B(t,T)) = D(t)\Big[- (\delta_0 + \delta_1 X_1 + \delta_2 X_2) f(t, X_1, X_2) + f_t(t, X_1, X_2) \tag{4.12}$$
$$+ (\mu_1 - \lambda_{11} X_1 - \lambda_{12} X_2) f_{x_1}(t, X_1, X_2) \tag{4.13}$$
$$+ (\mu_2 - \lambda_{21} X_1 - \lambda_{22} X_2) f_{x_2}(t, X_1, X_2) \tag{4.14}$$
$$+ \frac{1}{2} \sigma_1^2 X_1^{2\gamma_1} f_{x_1 x_1}(t, X_1, X_2) + \frac{1}{2} X_2^{2\gamma_2} f_{x_2 x_2}(t, X_1, X_2) \tag{4.15}$$
$$+ \rho \sigma_1 \sigma_2 X_1^{\gamma_1} X_2^{\gamma_2} f_{x_1 x_2}(t, X_1, X_2) \Big] dt \tag{4.16}$$
$$+ D(t)\Big[\sigma_1 X_1^{\gamma_1} f_{x_1} dW_1 + \sigma_2 X_2^{\gamma_2} f_{x_2} dW_2 \Big]. \tag{4.17}$$

Requiring the dt-term to be zero for all possible values of X_1, X_2, and t, we get the following partial differential equation for the function $f(t,x_1, x_2)$.

$$- (\delta_0 + \delta_1 x_1 + \delta_2 x_2) f + f_t + (\mu_1 - \lambda_{11} x_1 - \lambda_{12} x_2) f_{x_1} + (\mu_2 - \lambda_{21} x_1 - \lambda_{22} x_2) f_{x_2} + \tag{4.18}$$
$$+ \frac{1}{2} \sigma_1^2 x_1^{2\gamma_1} f_{x_1 x_1} + \frac{1}{2} \sigma_2^2 x_2^{2\gamma_2} f_{x_2 x_2} + \rho \sigma_1 \sigma_2 x_1^{\gamma_1} x_2^{\gamma_2} f_{x_1 x_2} = 0, \text{ for } x_1, x_2 \in \mathbb{R}^+, \ t \in [0,T] \tag{4.19}$$

Since $B(T,T) = 1$, we get the terminal condition $f(T, x_1, x_2) = 1$. If the two Brownian motions W_1 and W_2 are independent, $\rho = 0$ and there is thus no second order mixed derivative term in the PDE.

For the special case of the Vasicek model, $\gamma_1 = \gamma_2 = 0$ and the PDE reduces to

$$- (\delta_0 + \delta_1 x_1 + \delta_2 x_2) f + f_t + (\mu_1 - \lambda_{11} x_1 - \lambda_{12} x_2) f_{x_1} + (\mu_2 - \lambda_{21} x_1 - \lambda_{22} x_2) f_{x_2} + \tag{4.20}$$
$$+ \frac{1}{2} \sigma_1^2 f_{x_1 x_1} + \frac{1}{2} \sigma_2^2 f_{x_2 x_2} + \rho \sigma_1 \sigma_2 f_{x_1 x_2} = 0, \text{ for } x_1, x_2 \in \mathbb{R}, \ t \in [0,T]. \tag{4.21}$$

For the special case of the CIR model, $\gamma_1 = \gamma_2 = \frac{1}{2}$, and the PDE instead reduces to

$$-(\delta_0 + \delta_1 x_1 + \delta_2 x_2)f + f_t + (\mu_1 - \lambda_{11}x_1 - \lambda_{12}x_2)f_{x_1} + (\mu_2 - \lambda_{21}x_1 - \lambda_{22}x_2)f_{x_2} + \quad (4.22)$$

$$+\frac{1}{2}\sigma_1^2 x_1 f_{x_1x_1} + \frac{1}{2}\sigma_2^2 x_2 f_{x_2x_2} + \rho\sigma_1\sigma_2\sqrt{x_1x_2}f_{x_1x_2} = 0, \text{ for } x_1, x_2 \in \mathbb{R}^+, \ t \in [0,T]. \quad (4.23)$$

For the special case of the mixed model, we have $\gamma_1 = \frac{1}{2}$ and $\gamma_2 = 0$, and the PDE reduces to

$$-(\delta_0 + \delta_1 x_1 + \delta_2 x_2)f + f_t + (\mu_1 - \lambda_{11}x_1 - \lambda_{12}x_2)f_{x_1} + (\mu_2 - \lambda_{21}x_1 - \lambda_{22}x_2)f_{x_2} + \quad (4.24)$$

$$+\frac{1}{2}\sigma_1^2 x_1 f_{x_1x_1} + \frac{1}{2}\sigma_2^2 f_{x_2x_2} + \rho\sigma_1\sigma_2\sqrt{x_1}f_{x_1x_2} = 0, \text{ for } x_1 \in \mathbb{R}, \ x_2 \in \mathbb{R}^+, \ t \in [0,T]. \quad (4.25)$$

For the special case of the Rendleman-Bartter model, $\gamma_1 = \gamma_2 = 1$, and the PDE becomes

$$-(\delta_0 + \delta_1 x_1 + \delta_2 x_2)f + f_t + (\mu_1 - \lambda_{11}x_1 - \lambda_{12}x_2)f_{x_1} + (\mu_2 - \lambda_{21}x_1 - \lambda_{22}x_2)f_{x_2} + \quad (4.26)$$

$$+\frac{1}{2}\sigma_1^2 x_1^2 f_{x_1x_1} + \frac{1}{2}\sigma_2^2 x_2^2 f_{x_2x_2} + \rho\sigma_1\sigma_2 x_1x_2 f_{x_1x_2} = 0, \text{ for } x_1, x_2 \in \mathbb{R}, \ t \in [0,T]. \quad (4.27)$$

4.1.2 Affine yield models

An affine yield model is a model in which the pricing function $f(t,x_1,x_2)$ for a zero coupon bond takes the form

$$f(t, x_1, x_2) = e^{-x_1C_1(T-t) - x_2C_2(T-t) - A(T-t)}. \quad (4.28)$$

Recall that the yield of a zero coupon bond is the quantity $Y(t,T)$ such that $B(t,T) = e^{-Y(t,T)(T-t)}$. When the zero coupon bond price is given by a function of the form (4.28), the yield to maturity of a zero coupon bond is thus an affine function of the factors X_1 and X_2, and in turn of the interest rate. For this reason, the models where the pricing function is of the form (4.28) are collectively referred to as two-factor affine yield models. As will be discussed below, this ansatz separates the pricing PDE into a system of ODE for all parameter values in the special case of the Vasicek model. In the CIR and mixed models, the ansatz only works when $\rho = 0$. The Rendleman-Bartter model is not an affine yield model, since the ansatz (4.28) does not lead to a separation of variables in the pricing PDE for any parameter values.

Since the interest rate model parameters are not time-dependent, the price of the zero coupon bond only depends on T and t through $\tau = T - t$. We see that this is reflected in the choice of ansatz; the functions A, C_1 and C_2 only depend on T and t through τ.

Using the ansatz (4.28), the pricing PDE reduces to a system of coupled ODE for the functions $A(\tau)$, $C_1(\tau)$, and $C_2(\tau)$.

The first step in deriving this system of coupled ODE is to compute the partial derivatives of $f(t,x_1,x_2)$ in terms of A, C_1, and C_2:

$$f_t = \big(x_1C_1'(\tau) + x_2C_2'(\tau) + A'(\tau)\big)f \quad (4.29)$$

$$f_{x_1} = -C_1(\tau)f \tag{4.30}$$
$$f_{x_2} = -C_2(\tau)f \tag{4.31}$$
$$f_{x_1x_1} = C_1^2(\tau)f \tag{4.32}$$
$$f_{x_2x_2} = C_2^2(\tau)f \tag{4.33}$$
$$f_{x_1x_2} = C_1(\tau)C_2(\tau)f, \tag{4.34}$$

where $'$ denotes the derivative with respect to τ, and we have used the fact that

$$\frac{d}{dt}C_i(\tau) = -C_i'(\tau) \tag{4.35}$$
$$\frac{d}{dt}A(\tau) = -A'(\tau). \tag{4.36}$$

We also note that the terminal condition on f,

$$f(T,x_1,x_2) = e^{-x_1C_1(0)-x_2C_2(0)-A(0)} = 1, \tag{4.37}$$

implies the initial condition $A(0) = C_1(0) = C_2(0) = 0$ on the functions $A(\tau)$, $C_1(\tau)$ and $C_2(\tau)$.

The Vasicek model

We consider the PDE (4.20) for the Vasicek model first. Using the ansatz (4.28), the PDE becomes

$$f\big(-(\delta_0 + \delta_1x_1 + \delta_2x_2) + (x_1C_1'(\tau) + x_2C_2'(\tau) + A'(\tau)) \tag{4.38}$$
$$-(\mu_1 - \lambda_{11}x_1 - \lambda_{12}x_2)C_1(\tau) - (\mu_2 - \lambda_{21}x_1 - \lambda_{22}x_2)C_2(\tau) \tag{4.39}$$
$$+\frac{1}{2}\sigma_1^2C_1^2(\tau) + \frac{1}{2}\sigma_2^2C_2^2(\tau) + \rho\sigma_1\sigma_2C_1(\tau)C_2(\tau)\big) = 0. \tag{4.40}$$

Collecting terms in x_1 and x_2 we get

$$f\big((-\delta_1 + C_1'(\tau) + \lambda_{11}C_1(\tau) + \lambda_{21}C_2(\tau))x_1 + (-\delta_2 + C_2'(\tau) + \lambda_{12}C_1(\tau) + \lambda_{22}C_2(\tau))x_2 \tag{4.41}$$
$$+(-\delta_0 + A'(\tau) - \mu_1C_1(\tau) - \mu_2C_2(\tau) + \frac{1}{2}\sigma_1^2C_1^2(\tau) + \frac{1}{2}\sigma_2^2C_2^2(\tau) + \rho\sigma_1\sigma_2C_1(\tau)C_2(\tau)\big) = 0 \tag{4.42}$$

Noting that this equation must hold for all x_1 and x_2, we get a system of three simultaneous first order ordinary differential equations for the three functions C_1, C_2, and A in the ansatz:

$$C_1'(\tau) + \lambda_{11}C_1(\tau) + \lambda_{21}C_2(\tau) - \delta_1 = 0 \tag{4.43a}$$
$$C_2'(\tau) + \lambda_{12}C_1(\tau) + \lambda_{22}C_2(\tau) - \delta_2 = 0 \tag{4.43b}$$
$$A'(\tau) - \mu_1C_1(\tau) - \mu_2C_2(\tau) + \frac{1}{2}\sigma_1^2C_1^2(\tau) + \frac{1}{2}\sigma_2^2C_2^2(\tau) + \rho\sigma_1\sigma_2C_1(\tau)C_2(\tau) - \delta_0 = 0, \tag{4.43c}$$

where $\tau \in [0,T]$, and we recall the initial condition $A(0) = C_1(0) = C_2(0) = 0$.

We note that the function $A(\tau)$ only appears in the ODE (4.43c), and that both $C_1(\tau)$ and $C_2(\tau)$ and their derivatives appear in the first two ODE (4.43a)-(4.43b). Since the first two ODE are linear and have constant coefficients, they can be solved analytically. Since only the first derivative of $A(\tau)$ appears, the third equation can easily be integrated to obtain $A(\tau)$ once we know $C_1(\tau)$ and $C_2(\tau)$.

Thus we should start by solving the system of the two first (coupled) differential equations for $C_1(\tau)$ and $C_2(\tau)$.

In matrix form we have

$$C' + \Lambda^\top C = \delta \tag{4.44}$$

where

$$\Lambda^\top = \begin{pmatrix} \lambda_{11} & \lambda_{21} \\ \lambda_{12} & \lambda_{22} \end{pmatrix} \tag{4.45}$$

$$C = \begin{pmatrix} C_1(\tau) \\ C_2(\tau) \end{pmatrix} \tag{4.46}$$

$$\delta = \begin{pmatrix} \delta_1 \\ \delta_2 \end{pmatrix}. \tag{4.47}$$

The general solution to equation (4.44) is given by the general solution to the homogeneous problem plus a particular solution to (4.44). Since the right hand side is a constant vector, the particular solution can easily be found through the method of undetermined coefficients. Using the ansatz

$$C^p = \begin{pmatrix} \alpha_1 \\ \alpha_2 \end{pmatrix} \tag{4.48}$$

where α_1 and α_2 are real constants, and noting that $C^{p\prime}(\tau) = \begin{pmatrix} 0 \\ 0 \end{pmatrix}$, (4.44) gives

$$\Lambda^\top C^p = \delta \implies C^p = (\Lambda^\top)^{-1}\delta. \tag{4.49}$$

We note that the matrix inverse $(\Lambda^\top)^{-1}$ exists since $\Lambda^\top$ is the transpose of the matrix of drift coefficients of system of SDE. In chapter 3, we required that the matrix of drift coefficients Λ have strictly positive eigenvalues, which implies that its determinant must be strictly larger than zero[15]. This means that $\det(\Lambda^\top) > 0$ as well, and thus $\Lambda^\top$ is invertible.

It remains to find the general solution to

$$C' + \Lambda^\top C = \vec{0}. \tag{4.50}$$

or

$$C' = \tilde{\Lambda} C = -\Lambda^\top C \tag{4.51}$$

As long as the matrix $\tilde{\Lambda}$ has two distinct eigenvalues, it is guaranteed to have two linearly independent eigenvectors. In this case writing down the general solution to (4.51) is straightforward.

Denoting the eigenvectors of $\tilde{\Lambda}$ by $\tilde{\xi}^{(1)}$ and $\tilde{\xi}^{(2)}$, and the corresponding eigenvalues by $\tilde{r}_1$ and $\tilde{r}_2$, the general solution to the homogeneous problem is given by

$$c_1 e^{\tilde{r}_1 \tau}\tilde{\xi}^{(1)} + c_2 e^{\tilde{r}_2 \tau}\tilde{\xi}^{(2)}. \tag{4.52}$$

The general solution $C(\tau)$ to (4.44) is thus

$$C(\tau) = C^p + c_1 e^{\tilde{r}_1 \tau}\tilde{\xi}^{(1)} + c_2 e^{\tilde{r}_2 \tau}\tilde{\xi}^{(2)}, \tag{4.53}$$

where c_1 and c_2 are constants determined by the initial condition, and C^p is defined in equation (4.49). Recall that $C_1(\tau)$ and $C_2(\tau)$ are the components that make up the vector $C(\tau)$. Thus all that remains to do is to solve (4.43c) for the function $A(\tau)$, which is done through a straightforward integration.

The CIR model

Next, we consider the PDE (4.22) for the CIR model. Once again using the ansatz (4.28), the CIR PDE becomes

$$\begin{aligned} f\big(&- (\delta_0 + \delta_1 x_1 + \delta_2 x_2) + (x_1 C_1'(\tau) + x_2 C_2'(\tau) + A'(\tau)) && (4.54)\\ &- (\mu_1 - \lambda_{11}x_1 - \lambda_{12}x_2)C_1(\tau) - (\mu_2 - \lambda_{21}x_1 - \lambda_{22}x_2)C_2(\tau) && (4.55)\\ &+ \frac{1}{2}\sigma_1^2 x_1 C_1^2(\tau) + \frac{1}{2}\sigma_2^2 x_2 C_2^2(\tau) + \rho\sigma_1\sigma_2\sqrt{x_1 x_2}C_1(\tau)C_2(\tau)\big) = 0. && (4.56) \end{aligned}$$

Collecting terms in x_1 and x_2 we get

$$\begin{aligned} f\big(&(C_1'(\tau) + \lambda_{11}C_1(\tau) + \lambda_{21}C_2(\tau) + \frac{1}{2}\sigma_1^2 C_1^2(\tau) - \delta_1)x_1 + && (4.57)\\ &+ (C_2'(\tau) + \lambda_{12}C_1(\tau) + \lambda_{22}C_2(\tau) + \frac{1}{2}\sigma_2^2 C_2^2(\tau) - \delta_2)x_2 && (4.58)\\ &+ A'(\tau) - \mu_1 C_1(\tau) - \mu_2 C_2(\tau) - \delta_0 + \rho\sigma_1\sigma_2\sqrt{x_1 x_2}C_1(\tau)C_2(\tau)\big) = 0. && (4.59) \end{aligned}$$

If $\rho = 0$, similarly to in the Vasicek case, we get an expression only dependent on functions of τ multiplying x_1, another such expression multiplying x_1, and then a remaining expression only dependent on functions of τ. Requiring the equality to hold for all x_1 and x_2 in $\mathbb{R}^+$ we then get the following system of coupled ODE:

$$C_1'(\tau) + \lambda_{11}C_1(\tau) + \lambda_{21}C_2(\tau) + \frac{1}{2}\sigma_1^2 C_1^2(\tau) - \delta_1 = 0 \tag{4.60a}$$

$$C_2'(\tau) + \lambda_{12}C_1(\tau) + \lambda_{22}C_2(\tau) + \frac{1}{2}\sigma_2^2 C_2^2(\tau) - \delta_2 = 0 \tag{4.60b}$$

$$A'(\tau) - \mu_1 C_1(\tau) - \mu_2 C_2(\tau) - \delta_0 = 0, \tag{4.60c}$$

where again $\tau \in [0,T]$, and $A(0) = C_1(0) = C_2(0) = 0$.

As opposed to in the Vasicek case, these ODE are not linear, so we cannot proceed in the same way to get an analytical solution. The ODE can however be solved numerically.

The mixed model

We also consider the PDE (4.24) for the mixed model. Using the ansatz (4.28), the mixed model PDE becomes

$$
\begin{aligned}
&f\big(-(\delta_0 + \delta_1 x_1 + \delta_2 x_2) + (x_1 C_1'(\tau) + x_2 C_2'(\tau) + A'(\tau)) && (4.61)\\
&\quad -(\mu_1 - \lambda_{11} x_1 - \lambda_{12} x_2) C_1(\tau) - (\mu_2 - \lambda_{21} x_1 - \lambda_{22} x_2) C_2(\tau)) && (4.62)\\
&\quad + \frac{1}{2}\sigma_1^2 x_1 C_1^2(\tau) + \frac{1}{2}\sigma_2^2 C_2^2(\tau) + \rho\sigma_1\sigma_2\sqrt{x_1} C_1(\tau) C_2(\tau)\big). && (4.63)
\end{aligned}
$$

Collecting terms in x_1 and x_2 we get

$$
\begin{aligned}
&f\big((C_1'(\tau) + \lambda_{11} C_1(\tau) + \lambda_{21} C_2(\tau) + \sigma_1^2 C_1^2(\tau) - \delta_1) x_1 && (4.64)\\
&\quad + (C_2'(\tau) + \lambda_{12} C_1(\tau) + \lambda_{22} C_2(\tau) - \delta_2) x_2 && (4.65)\\
&\quad + A'(\tau) - \mu_1 C_1(\tau) - \mu_2 C_2(\tau) + \frac{1}{2}\sigma_2^2 C_2^2(\tau) - \delta_0 + \rho\sigma_1\sigma_2\sqrt{x_1} C_1(\tau) C_2(\tau)\big) = 0. && (4.66)
\end{aligned}
$$

As in the CIR case, when $\rho = 0$, we get an expression only dependent on functions of τ multiplying x_1, another such expression multiplying x_2, and then a remaining expression only dependent on functions of τ. Requiring the equality to hold for all $x_1 \in \mathbb{R}$ and all $x_2 \in \mathbb{R}^+$, we then get the following system of coupled ODE:

$$
\begin{aligned}
&C_1'(\tau) + \lambda_{11} C_1(\tau) + \lambda_{21} C_2(\tau) + \sigma_1^2 C_1^2(\tau) - \delta_1 = 0 && (4.67a)\\
&C_2'(\tau) + \lambda_{12} C_1(\tau) + \lambda_{22} C_2(\tau) - \delta_2 = 0 && (4.67b)\\
&A'(\tau) - \mu_1 C_1(\tau) - \mu_2 C_2(\tau) + \frac{1}{2}\sigma_2^2 C_2^2(\tau) - \delta_0 = 0, && (4.67c)
\end{aligned}
$$

where again $\tau \in [0,T]$, and $A(0) = C_1(0) = C_2(0) = 0$. As in the CIR model case, the ODE can be solved numerically.

4.2 Numerical Methods

As discussed in section 4.1, one way to price zero coupon bonds in the specified two-factor interest rate models is by solving the pricing PDE, which in the case of affine yield models reduces to a system of ODE. While partial differential equations can in some cases be complicated to solve numerically, and require different methods depending on the type of PDE, ordinary differential equations tend to be easy and not too computationally intense to solve numerically. Thus the ODE method of ZCB pricing is a good choice when applicable.

Another method for pricing zero coupon bonds in the specified interest rate models is to directly estimate the expectation in the risk-neutral pricing formula using Monte-Carlo methods. Whilst Monte-Carlo methods are quite computationally expensive, they are very general, requiring little modification to work for different interest rate models and different parameter values. For example, Monte-Carlo methods can be used to price ZCBs in the two factor CIR and mixed interest rate models even when the correlation ρ between the two Brownian motions is nonzero, and for other values of the parameters γ_1 and γ_2 in the general two-factor interest rate model discussed in this thesis. The specifics of the Monte-Carlo methods used are outlined below.

4.2.1 Monte-Carlo Methods

The aim is to approximate the expectation in the risk-neutral pricing formula

$$B(t,T) = \tilde{\mathbb{E}}\big[e^{-\int_t^T R(s)ds} \mid \mathcal{F}(t)\big], \tag{4.68}$$

using Monte-Carlo methods. Since the interest rate $R(t)$ is a function of the factors $X_1(t)$ and $X_2(t)$, which are homogeneous Markov processes, the price $B(t,T)$ of a zero coupon bond in the model will only depend on the time left to maturity, $\tau = T - t$[16]. Thus it is enough to consider the prices of zero coupon bonds at time zero with varying maturities, since $B(t,T) = B(0,T-t)$. We thus only need to consider the simpler form of the risk-neutral pricing formula

$$B(0,T) = \tilde{\mathbb{E}}\big[e^{-\int_0^T R(s)ds}\big]. \tag{4.69}$$

The simplest Monte-Carlo estimator for the expectation of a random variable Y is the empirical mean,

$$\overline{Y}_M = \frac{1}{M}\sum_{m=1}^{M} Y_m, \tag{4.70}$$

which converges to $\mathbb{E}[Y]$ as $M \to \infty$ by the law of large numbers.

In this case $Y = e^{-\int_0^T R(s)ds}$, and we have

$$\overline{Y}_M = \sum_{m=1}^{M} e^{-\int_0^T R_m(s)ds} \tag{4.71}$$

To estimate the zero coupon bond price numerically, one thus needs to compute many (discretised) paths of the interest rate $R(t)$, and then approximate the integral $\int_0^T R(s)ds$. The former is done using an Euler-Maruyama discretisation scheme for the system of SDE (4.1), as outlined in section 3.2.1. The latter is done simply by approximating the integral as a right Riemann sum, which in practice just involves summing up the values of $R(t)$ along a discretised path simulated using the Euler-Maruyama scheme. Thus the approximation of (4.69) with uniform timestep h and number of Monte-Carlo simulations M is given by

$$\overline{Y}_M^h = \sum_{m=1}^{M} e^{-\sum_i R(s_i)h} \tag{4.72}$$

We note that there are two sources of error in the numerical simulation; the size of the timestep h in the Euler-Maruyama scheme, and the non-infinite number of paths M used to approximate the expectation. To get a more accurate price, one can decrease the timestep h or increase the number of paths M.

Another method that can be used is the multi-level Monte-Carlo method, where one approximates expectations at different levels, where the timestep varies with each level. The method utilises the linearity of expectation to get the telescoping sum

$$\mathbb{E}[Y^{h_L}] = \mathbb{E}[Y^{h_0}] + \sum_{l=1}^{L} \mathbb{E}[Y^{h_l} - Y^{h_{l-1}}]. \tag{4.73}$$

Here, Y^{h_l} denotes the Euler-Maruyama scheme approximation of $e^{-\int_0^T R(s)ds}$ with timestep h_l. The expectations in the above expression are then approximated as sums, yielding the multi-level Monte-Carlo estimator

$$\overline{Y}^{h_0,\dots h_L}_{M_0,\dots,M_L} = \sum_{m=1}^{M_0} Y_m^{h_0} + \sum_{l=1}^{L} \sum_{m=1}^{M_l} (Y_m^{h_l} - Y_m^{h_{l-1}}). \tag{4.74}$$

The main idea of the Multilevel Monte-Carlo method, is to reduce the computational cost of reaching a certain accuracy. Instead of directly computing the Monte-Carlo estimator with a very fine time step h and a very large number of simulations M, computations are carried out on a number of levels, with increasingly smaller time step h_l and decreasing number of simulations M_l. It is important to note that for each term in the inner sum, the two discretised paths $Y_m^{h_l}$ and $Y_m^{h_{l-1}}$ at the same level l must be generated using the same path of the driving noise, but at different levels of coarseness.

Because of this, the method relies on our ability to simulate the same path at different levels of coarseness - i.e. with the different time steps h_l and h_{l-1}. We can do this because it is possible to generate the same path of the driving noise - the Brownian motion - at different levels of coarseness. For example, this can be done by first generating a Brownian motion path with the smaller time step h_l, and then sampling every other point of it to get the coarser path with time step h_{l-1}[8].

Since the modified Euler-Maruyama scheme introduced in [14] relies on random numbers with a different distribution, and also only guarantees weak conversion, there is no guarantee that the multi-level Monte-Carlo method will work along with this method. Thus, we use the regular (non-multi-level) Monte-Carlo estimator together with the scheme [14], and the multi-level Monte-Carlo estimator for the other versions of the Euler-Maruyama scheme.

Comparisons of the numerical zero coupon bond prices achieved using Monte-Carlo methods and using ODE methods, are presented in the next section.

4.2.2 Numerical Comparison of Zero Coupon Bond Prices

In this section, the zero coupon bond prices obtained using different numerical methods are compared for the two-factor Vasicek, CIR, and mixed models.

As previously discussed, the ODE approach works for all parameter values in the Vasicek model, and thus we can always obtain zero coupon bond prices in the model by solving the system of ODE (4.43). In figure 4.1, the ZCB prices obtained by solving the system (4.43) using the MatLab function `ode45`, are compared with the prices obtained using an Euler-Maruyama scheme in combination with the multi-level Monte-Carlo method. Prices are compared for maturities ranging from 1 to 20 years, and in three cases; for negative, positive, and zero correlation ρ. As can be seen from figure 4.1, the prices obtained from the two numerical methods agree very well in all three cases.

In the CIR model and the mixed model, we can obtain zero coupon bond prices by using the ODE approach only when the correlation ρ between the two Brownian motions is zero. For these two models, the prices obtained using the ODE approach and the Monte-Carlo approach are thus compared only in the case $\rho = 0$. As discussed previously, in order to

overcome the problem of maintaining positivity, two different modifications of the Euler-Maruyama scheme for the CIR and mixed models are used in this thesis. The ZCB prices obtained using these two methods, the symmetrized Euler-Maruyama scheme in combination with the multi-level Monte-Carlo method, and the scheme suggested in [14] in combination with the regular Monte-Carlo method, are both compared to the ZCB prices obtained using the ODE approach. As in the Vasicek case, the systems of ODE are solved numerically using the MatLab function `ode45`.

In the case of the CIR model, the system of ODE to be solved is (4.60). Comparisons of ZCB prices obtained using the different numerical methods are presented in figure 4.2. It can be seen that the ZCB prices obtained using both versions of Monte-Carlo methods agree well with the prices obtained using the ODE approach.

For the mixed model, the system of ODE to be solved is (4.67), and ZCB price comparisons are presented in figure 4.3. As in the CIR model case, the ZCB prices obtained using the two different versions of Monte-Carlo methods agree well with the prices obtained using the ODE approach.

In summary, the Monte-Carlo prices agree with the ODE prices for all values of ρ in the Vasicek model. The prices also agree in the CIR and mixed models when it is possible to compute prices using the ODE approach - i.e. when $\rho = 0$. We take this as an indication that the prices obtained using Monte-Carlo methods for the CIR and mixed models should be reliable also when $\rho \neq 0$. Furthermore, both of the adjusted Euler-Maruyama schemes for the CIR and mixed models seem equally reliable.

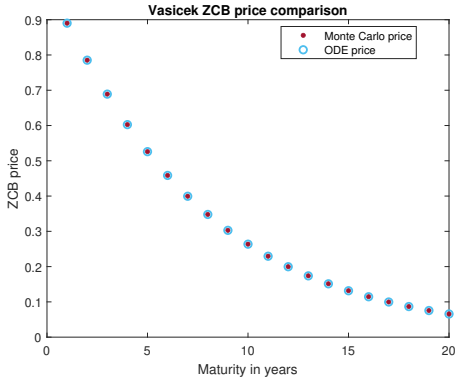

(a) Comparison of zero coupon bond prices in the Vasicek model. Here, the correlation ρ between the two Brownian motions is negative, $\rho = -0.9$.

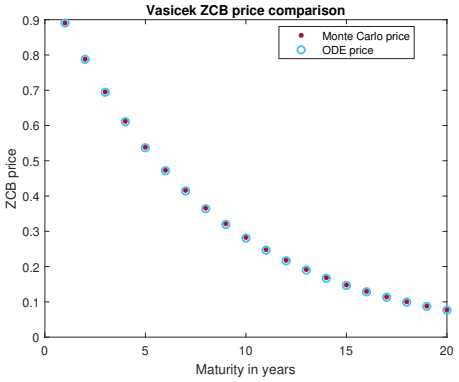

(b) Comparison of zero coupon bond prices in the Vasicek model. Here, the correlation ρ between the two Brownian motions is zero.

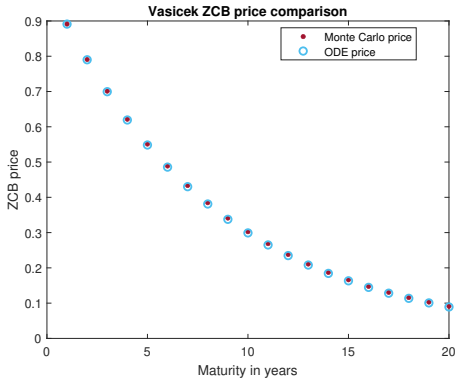

(c) Comparison of zero coupon bond prices in the Vasicek model. Here, the correlation ρ between the two Brownian motions is positive, $\rho = 0.9$.

Figure 4.1: Zero coupon bond price comparisons in the two-factor Vasicek model. It can be seen that the prices obtained using Monte-Carlo simulation agree well with the prices obtained using the ODE method, for both positive, negative, and zero correlation ρ.

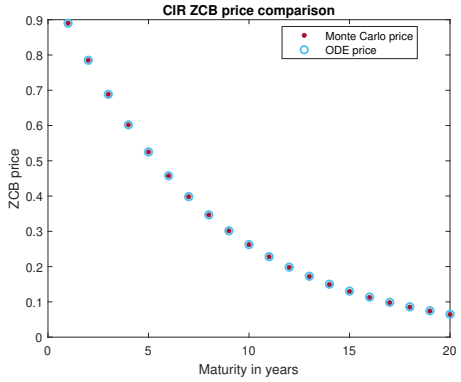

(a) Comparison of zero coupon bond prices in the two-factor CIR model. Here, the Monte-Carlo prices are obtained using the symmetrized Euler-Maruyama scheme in combination with the multi-level Monte-Carlo method. The correlation between the two Brownian motions, $\rho = 0$.

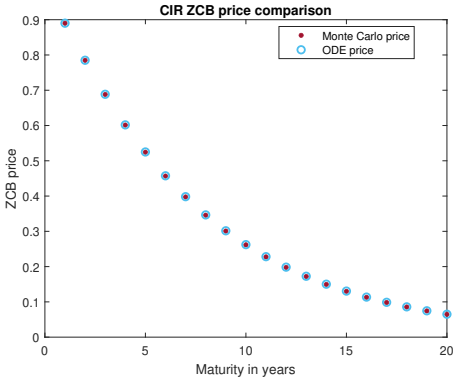

(b) Comparison of zero coupon bond prices in the two-factor CIR model. Here, the Monte-Carlo prices are obtained using the modified Euler-Maruyama scheme suggested in [14] in combination with a the regular Monte-Carlo method. The correlation between the two Brownian motions, $\rho = 0$.

Figure 4.2: Zero coupon bond price comparisons in the two-factor CIR model. It can be seen that the prices obtained using Monte-Carlo methods agree well with the prices obtained using the ODE method, for both the symmetrized Euler-Maruyama scheme and the alternative scheme suggested in [14].

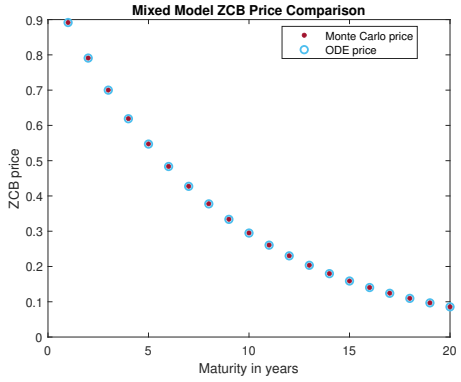

(a) Comparison of zero coupon bond prices in the two-factor mixed model. Here, the Monte-Carlo prices are obtained using the symmetrized Euler-Maruyama scheme in combination with the multi-level Monte-Carlo method. The correlation between the two Brownian motions, $\rho = 0$.

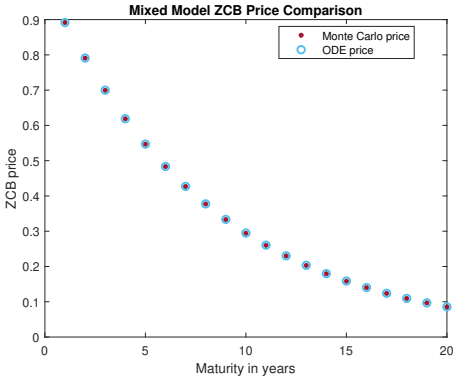

(b) Comparison of zero coupon bond prices in the two-factor mixed model. Here, the Monte-Carlo prices are obtained using the modified Euler-Maruyama scheme suggested in [14] in combination with a the regular Monte-Carlo method. The correlation between the two Brownian motions, $\rho = 0$.

Figure 4.3: Zero coupon bond price comparisons in the two-factor mixed model. Similarly to in the case of the CIR model, we see that that the prices obtained using Monte-Carlo methods agree well with the prices obtained using the ODE method for both the symmetrized Euler-Maruyama scheme and the weak scheme suggested in [14].

4.2.3 Comparison of ZCB Prices with Different Correlation

In this section, we compare the zero coupon bond prices in the different interest rate models when varying the correlation ρ between the two Brownian motions in each model, while keeping all other parameters constant. We find that the prices vary significantly with correlation only in the Vasicek model. The results are plotted in figure 4.4

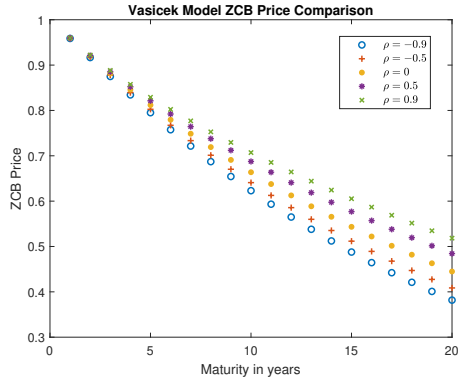

(a) Zero coupon bond prices for different values of correlation ρ in the two factor Vasicek model.

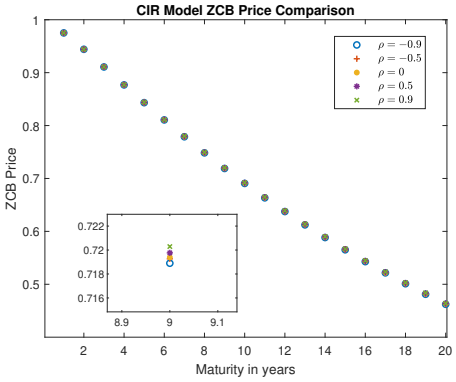

(b) Zero coupon bond prices for different values of correlation ρ in the two factor CIR model. In the smaller plot, a zoomed in view is shown.

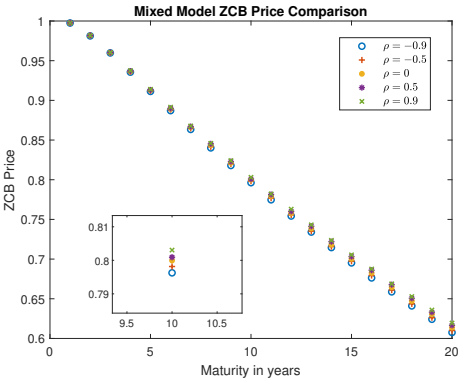

(c) Zero coupon bond prices for different values of the correlation ρ in the two factor mixed model. In the smaller plot, a zoomed in view is shown.

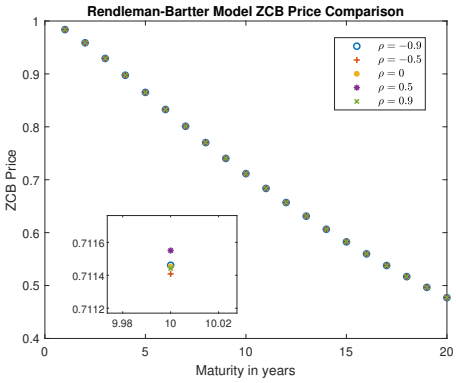

(d) Zero coupon bond prices for different values of the correlation ρ in the two factor Rendleman-Bartter model. In the smaller plot, a zoomed in view is shown.

Figure 4.4: Comparison of zero coupon bond prices in the different two factor interest rate models that we investigate. The prices of zero coupon bonds with maturities from one to 20 years are plotted for different values of ρ. In each plot, the only parameter that has been varied is the correlation ρ between the two Brownian motions, whilst all other parameters have been kept constant. It can be seen that there is only a significant change in the zero coupon bond values with ρ in the two factor Vasicek model.

4.2.4 Comparison of ZCB Prices in Different Interest Rate Models

In this section, we compare zero coupon bond prices in the different interest rate models, with prices in all models plotted on the same axes. These plots can be seen below in figure 4.5.

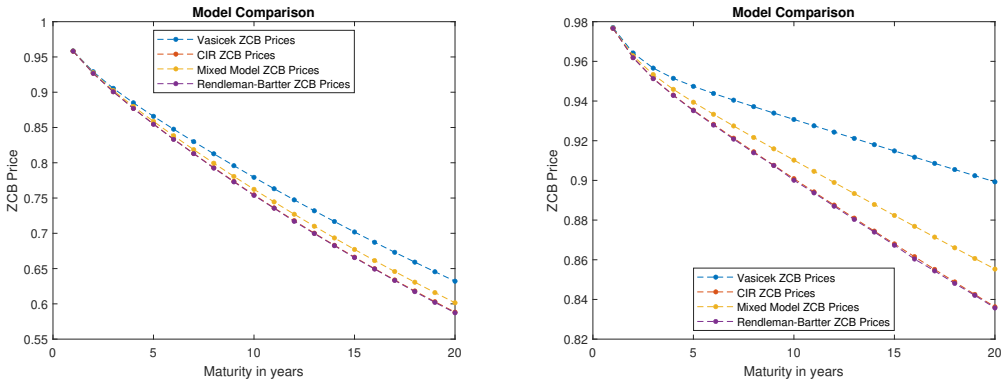

Figure 4.5: Comparison of zero coupon bond prices in the four investigated interest rate models. We see that the ZCB prices do indeed differ. Note the scale on the axes in the plot on the right.

5

Yield curves

5.1 Theory

5.1.1 Interpretation of yield curve shapes

Depending on the relationship between short term yields and long term yields, the shape of the yield curve is described as either normal, steep, inverted, or flat[17]. The fact that the yields to maturity of bonds with different maturities are not normally all equal implies that there are different costs and levels of risk associated with investing in bonds with different maturities[6].

The normal yield curve is the shape most commonly seen in markets. In the normal yield curve, bonds with shorter maturities have a lower yield than bonds with longer maturities. For very long maturities, the curve tends to flatten out. This is the shape that the yield curve tends to take under normal, stable economic conditions.

In a steep yield curve, like in a normal yield curve, the yields to maturity of bonds with longer maturities are higher than those of bonds with shorter maturities. The main difference between the two shapes is that a steep yield curve, as the name implies, has a steeper slope than a normal yield curve. The steep yield curve also does not tend to flatten out at higher maturities as much as a normal yield curve does, if at all[17]. Historically, steep yield curves have often been seen before periods of significant economic growth, when both inflation and interest rates tend to be higher.

In an inverted yield curve, the yields to maturity of bonds with longer maturities are lower than those of bonds with shorter maturities. The curve also tends to flatten out for the longest maturities. Inverted yield curves only occur rarely in modern markets, and then have often been observed before a significant slowdown in the economy, such as right at the start of a recession[17].

The flat or humped yield curve is also quite rare. In a flat yield curve, the yields of bonds are the same for all maturities, varying by at most the order of 0.01 och 0.1 percent. In a humped yield curve, the flat curve has a bump for medium maturities, where yields are slightly higher or lower. Flat or humped yield curves have historically appeared in times of high economic uncertainty, for example when a period of significant economic growth is coming to an end[17].

Different models have been suggested to explain the different shapes that the yield curve takes. According to the expectations hypothesis, the shape of the yield curve reflects what the market and its investors expect will happen with interest rate levels in the future[6]. There are different versions of the expectations hypothesis; for example the unbiased expectations hypothesis, the return to maturity expectations hypothesis, the yield to maturity expectations hypothesis, and the local expectations hypothesis. Mathematically, the different versions are quite different, but as far as qualitative interpretation of the yield curve

goes, they are all based on the premise of market expectations regarding the interest rate. According to the hypothesis, an inverted yield curve suggests that investors expect interest rates to fall in the future. When investors expect lower interest rates in the future, they will favour buying bonds with long maturities to "lock in" the higher yields associated with these bonds today. This increase in demand for bonds with long maturities will push up the prices of these bonds, leading to them having lower yields to maturity than the less desirable bonds with shorter maturities. Similarly, if short-term interest rates are expected to rise, bonds with shorter maturities will be less desirable than bonds with longer maturities. This increased demand leads to higher prices for short term bonds, which in turn means their yield to maturity is lower than the yield to maturity of longer term bonds[6].

Another model for explaining the shapes that the yield curve takes is so called liquidity preference theory. This theory is based on the observation that investors tend to favour investments with higher liquidity, i.e. which can more easily be converted into cash. In the bond market, this is bonds which have shorter maturities, as holding a series of shorter term bonds one after the other provides more flexibility than holding one longer term bond. The default state of the market is then assumed to be that bonds with longer maturities have higher yields than bonds with shorter maturities, as a sort of premium or compensation for an investor that chooses to invest in the less liquid longer term bonds. Another way to think of this is in terms of interest rates, where a longer term loan tends to be offered at a higher interest rate than a shorter term loan, as there are more risks associated with lending someone money for a longer period of time[6]. For example, offering someone a longer term loan, there is a higher risk of them going bankrupt in the time before the loan is to be paid back.

Liquidity preference theory explains why the yield curve shape most commonly seen in markets is the normal yield curve, rather than the flat yield curve. The theory attributes the normal yield curve shape to investors tending to prefer shorter term bonds, both as there is less risk associated with them, and as they are a more liquid asset[6].

Another theory is provided by the segmentation hypothesis, which can be used to explain all shapes that the yield curve can take, but which does not offer any interpretation of the yield curve shape on its own[6]. The hypothesis is based on the fact that different types of investors have different needs – for example, banks have a need for short term bonds whereas insurance companies and pension funds have a need for long term bonds. For these types of investors, a long term bond and a short term bond are not exchangeable, which according to the segmentation hypothesis segments the market. A market being segmented means that there is little connection between the prices and supply and demand of shorter term bonds and that of longer term bonds. According to the segmentation hypothesis, a flat and humped yield curve could be explained by there being an equally high demand – but from different types of investors – for short and long maturity bonds, but less of a demand for medium term bonds. This would then lower the prices of medium term bonds, which leads to their yields to maturity being higher compared to those of short and long term bonds[6]. A modified version of the segmentation hypothesis, called preferred habitat theory, operates of the same premise, but recognises that there is some flexibility in which bonds investors choose to invest in.

At any given time, the shape of the yield curve is most likely to not be explained by any one of these theories alone, but rather by a combination of them[6].

5.1.2 Calculating the yield to maturity

As stated previously, since the factors that make up the interest rate are homogeneous Markov processes, the prices of bonds in the interest rate models we consider will only depend on the time left to maturity, and thus it is enough to consider the prices of bonds with different maturities at time zero. We thus consider the yield to maturity $Y_c(0,T)$ at

time zero of coupon bonds with different maturities T. For a coupon bond that pays coupons $\{c_1,...,c_N\}$ at times $\{t_1,...,t_N\}$ the yield to maturity $Y_c(0,T)$ solves the equation

$$\sum_{i=1}^{N-1} c_i e^{-Y_c(0,T)t_i} + (1+c_N)e^{-Y_c(0,T)T} - B_c(0,T) = 0. \tag{5.1}$$

If time is measured in years, and we let both the maturity of the bond and all times at which a coupon is paid be integer numbers of years, equation (5.1) becomes a polynomial equation for $x = e^{-Y_c(0,T)}$ of the form

$$\sum_{k=1}^{N-1} c_k x^k + (1+c_N)x^N - B_c(0,T) = 0. \tag{5.2}$$

Since we are mainly interested in qualitative properties of the yield curve, like its overall shape, this is a reasonable simplification to make. It is straightforward to find the roots of any polynomial numerically, and we do this using the MatLab function `roots`.

In general, an N^{th} degree polynomial has multiple distinct roots, so it is important to consider how to choose between these roots. For the yield to maturity to have any real-world meaning, it must be a real number. Since the yield is given in terms of the variable x as $Y_c(0,T) = -\ln x$, we are thus only interested in real, positive solutions to the polynomial equation (5.2). Clearly all coupons $c_1,...,c_N$ must be positive, meaning that all coefficients of the polynomial on the left hand side of (5.2) are positive, except possibly the constant term coefficient. Furthermore, the price $B_c(0,T)$ of the coupon bond should also be positive, meaning that the quantity $-B_c(0,T)$ is negative. Thus, there is a total of one coefficient sign change in the polynomial, which by Descartes' rule of signs means that the polynomial has exactly one positive real root. Thus, there is no ambiguity in the choice of polynomial root from which to compute $Y_c(0,T)$.

5.1.3 Choice of Coupon Values

As stated previously, we can without loss of generality restrict to studying coupon bonds with face value 1. However, we still need to specify the values of the coupons $\{c_1,...,c_N\}$ that the coupon bonds pay. Typically, all the coupons that a given coupon bond pays are equal [5], and this is the case that we will consider here as well. However, it is common that coupon bonds with different maturities offer different coupons, see for example the bonds offered by the Swedish National Debt Office [1] or the bonds offered by the US Treasury [3]. It is common for the coupons to increase with the maturity of the bond. Here, we will take inspiration mainly from the coupons offered on US Treasury Notes and Treasury Bonds with maturities 2, 5, 10, and 30 years. The data used was retrieved from Bloomberg.com on 29^{th} January 2021, when the coupons were 0.13, 0.38, 0.88, and 1.63 percent respectively.

In our numerical investigations, we plot yield curves for coupon bonds with maturities from 1 to 20 years, and to get reasonable coupon values for the intermediate maturities, we use linear interpolation, specifically the MatLab function `interp1`.

5.2 Numerical Results

We present results in terms of numerically generated yield curves in the studied interest rate models. We successfully recreate the four main shapes – normal, steep, inverted, and flat – that the yield curve can take in the two-factor Vasicek model, CIR model, mixed model, and Rendleman-Bartter model. We also compare the yield curves obtained in the different models with the same parameter values.

5.2.1 Recreation of Yield Curve Shapes in Different Interest Rate Models

In figure 5.1, yield curves generated numerically in the two-factor Vasicek, CIR, mixed, and Rendleman-Bartter models can be seen. The four main yield curve shapes; normal, steep, inverted, and flat have all been reproduced. In all models, a normal yield curve could be reproduced when the initial value of the interest rate was smaller than the mean-reversion value, an inverted yield curve could be reproduced when the initial value was larger than the mean-reversion value, and a flat yield curve when the two values were roughly equal. To reproduce a steep yield curve, we also chose an initial value smaller than the mean-reversion value, and a matrix of coefficients Λ with smaller eigenvalues.

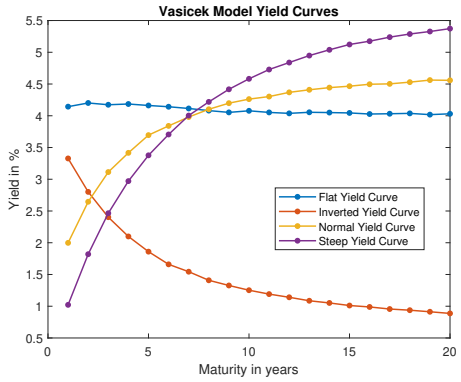

(a) Yield curve shapes in the two-factor Vasicek model.

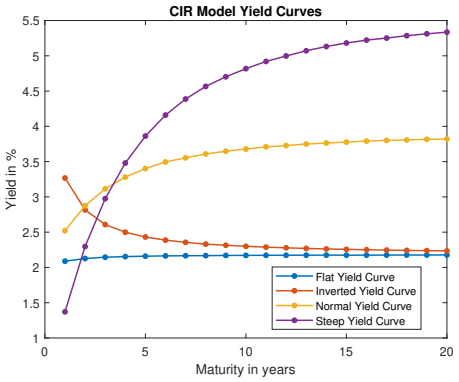

(b) Yield curve shapes in the two-factor CIR model.

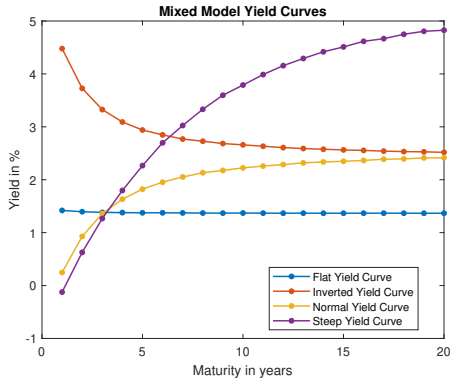

(c) Yield curve shapes in the two-factor mixed model.

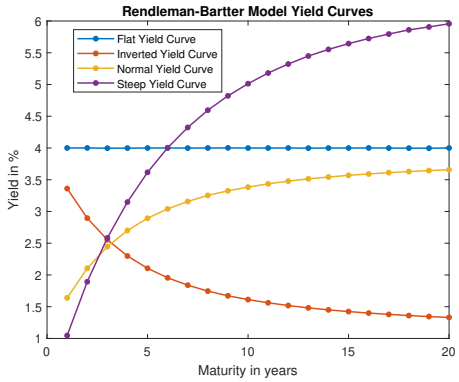

(d) Yield curve shapes in the two-factor Rendleman Bartter model.

Figure 5.1: Recreation of the four main yield curve shapes – normal, steep, inverted, and flat or humped – in the two-factor Vasicek, CIR, mixed, and mean-reverting Rendleman-Bartter models.

5.2.2 Comparison of Yield Curves In Different Models

In figure 5.2, comparisons of yield curves in the two factor Vasicek model, CIR model, mixed model and Rendleman-Bartter model can be seen.

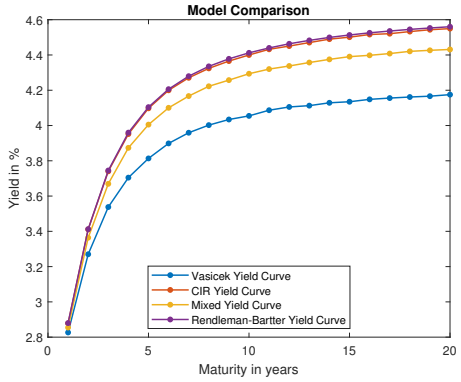

(a) Comparison of normal yield curves in the two-factor Vasicek model, CIR model, mixed model, and Rendleman-Bartter model.

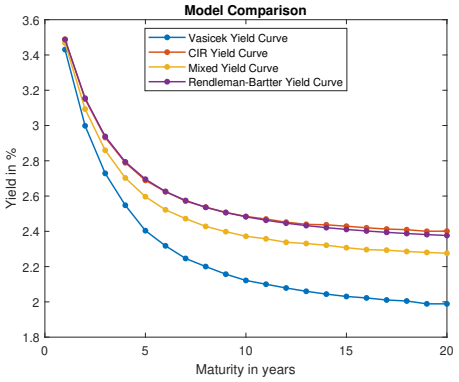

(b) Comparison of inverted yield curves in the two-factor Vasicek model, CIR model, mixed model, and Rendleman-Bartter model.

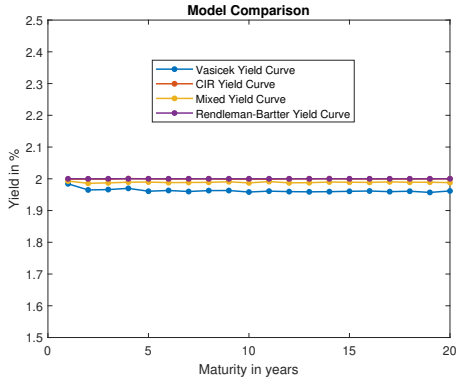

(c) Comparison of flat yield curves in the two-factor Vasicek model, CIR model, mixed model, and Rendleman-Bartter model.

Figure 5.2: Comparison of yield curves in the two-factor Vasicek model, CIR model, mixed model and Rendleman-Bartter model. In each figure, the parameter values are the same for the yield curves from all the models, with the only difference being in the model determining parameters γ_1 and γ_2. At least for the chosen parameter values, the three models all produce the same shape when their parameter values are the same. In the case of the normal and inverted yield curves, the numerical values of the yield to maturity differ significantly between the models.

5.2.3 Comparison of Yield Curves with Different Correlation

In figure 5.3, comparisons of yield curves in the two-factor Vasicek model, CIR model, mixed model, and Rendleman-Bartter model for different values of correlation ρ between the two Brownian motions can be seen. As is expected from the comparisons of zero coupon bond prices with varying ρ in figure 4.4, the values of the yield to maturity only vary considerably with ρ in the Vasicek model.

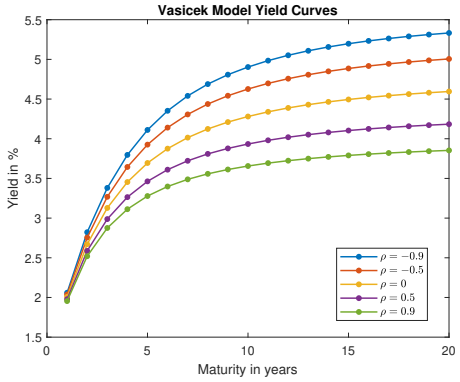

(a) Yield curves in the two-factor Vasicek model for different values of correlation ρ between the Brownian motions in the model.

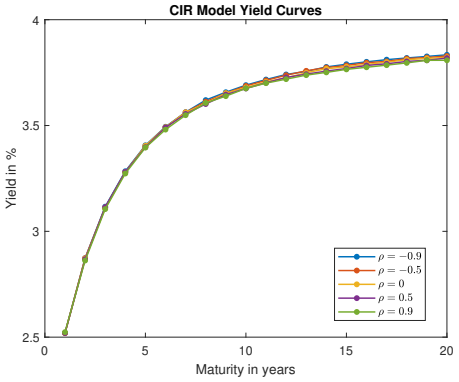

(b) Yield curves in the two-factor CIR model for different values of correlation ρ between the Brownian motions in the model.

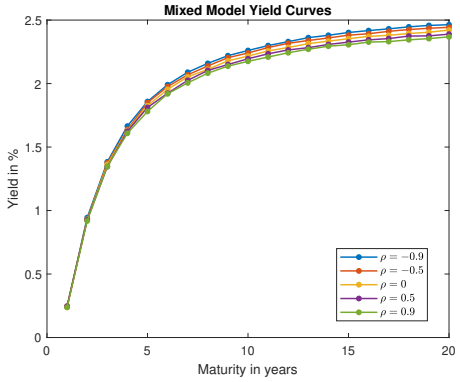

(c) Yield curves in the two-factor mixed model for different values of correlation ρ between the Brownian motions in the model.

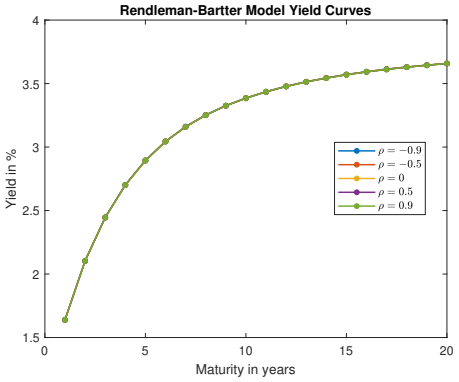

(d) Yield curves in the two-factor Rendleman-Bartter model for different values of correlation ρ between the Brownian motions in the model.

Figure 5.3: Comparison of yield curves with varying correlation ρ between the two Brownian motions in each interest rate model. Yield curves with all parameters kept constant except ρ are plotted in the two-factor Vasicek model, CIR model, mixed model, and Rendleman-Bartter model. There is only a significant change in the yield to maturity with changing correlation ρ in the two-factor Vasicek model.

5.2.4 Recreating Normal Yield Curves with Negative Yield for Short Maturities

Currently, the yield to maturity for coupon bonds with shorter maturities offered by the Swedish National Debt Office is slightly negative, while the yield to maturity for longer term coupon bonds is positive[1]. This is a motivation for investigating whether we can recreate a normal yield curve that starts off negative in the interest rate models that we investigate. In 5.4 yield curves that fit this description are plotted.

In all models except the two-factor CIR model, it is possible to recreate a normal yield curve that is negative for low maturities by letting the initial value of the interest rate be negative, and letting the mean-reversion value be positive. This approach does not work for the CIR model, since the conditions for existence and uniqueness for the CIR SDE state that the initial condition must be strictly positive. However, it is still possible to recreate

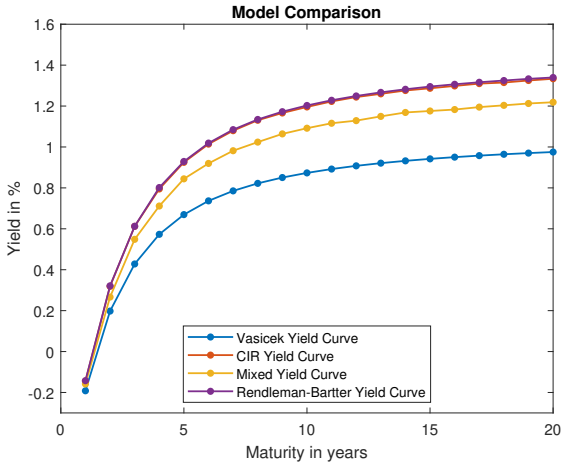

Figure 5.4: Normal yield curves in the Vasicek, CIR, mixed, and Rendleman-Bartter models where the yield to maturity is negative for short maturities.

a yield curve that is negative at the start in the two-factor CIR model by choosing the parameters δ_0, δ_1, and δ_2 that determine how the interest rate depends on the factors $X_1(t)$ and $X_2(t)$. If we choose δ_0 sufficiently negative, or indeed if we choose one or both of δ_1 and δ_2 negative, the interest rate will be negative even though the factors $X_1(t)$ and $X_2(t)$ are strictly positive for all t. In this case, a yield curve that is negative for short maturities can be recreated. This approach can naturally be used to reproduce negative yields in the other interest rate models as well. However, we note that if we impose that the parameters δ_0, δ_1, and δ_2 must be greater than zero – which we would do in the CIR model to ensure that not just the factors X_1 and X_2 but also the interest rate remains positive – it does not seem possible to recreate negative yields to maturity in the CIR model.

5.2.5 Mixed Model Comparison

In the two-factor mixed model, one factor follows a CIR model and one factor follows a Vasicek model. The interest rate is then a weighted average of a one dimensional CIR process and a one dimensional Vasicek process. In figure 5.5, comparisons of yield curves with different weights given to the CIR factor and the Vasicek factor can be seen.

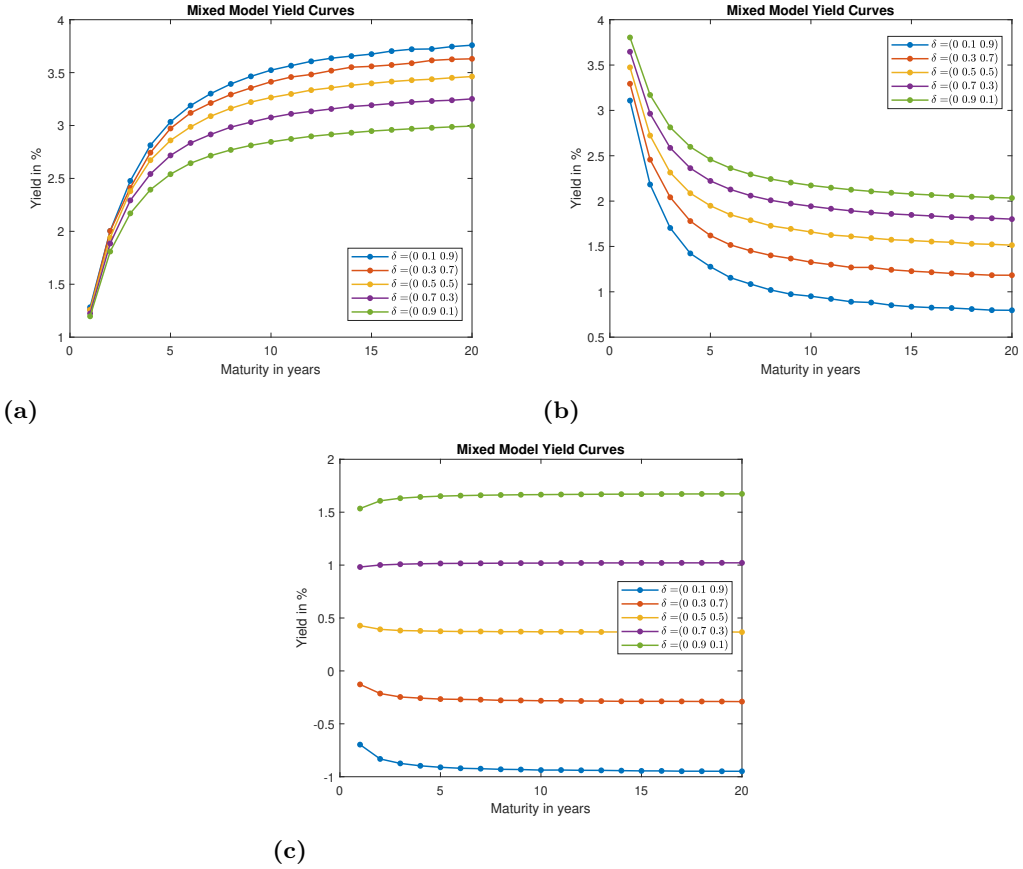

Figure 5.5: Comparison of yield curves in the mixed model with different weight given to the Vasicek factor and the CIR factor. Note that the interest rate is given by $R(t) = \delta_0 + \delta_1 X_1(t) + \delta_2 X_2(t)$, where $X_1(t)$ is the CIR process, and $X_2(t)$ is the Vasicek process.

5.2.6 Rendleman-Bartter Model Without Mean Reversion

We present a few yield curves from the two-factor Rendleman-Bartter model for parameter values where the interest rate is not mean-reverting in figure 5.6. The yield curve does not flatten out for large maturities, as it does when the interest rate is mean-reverting.

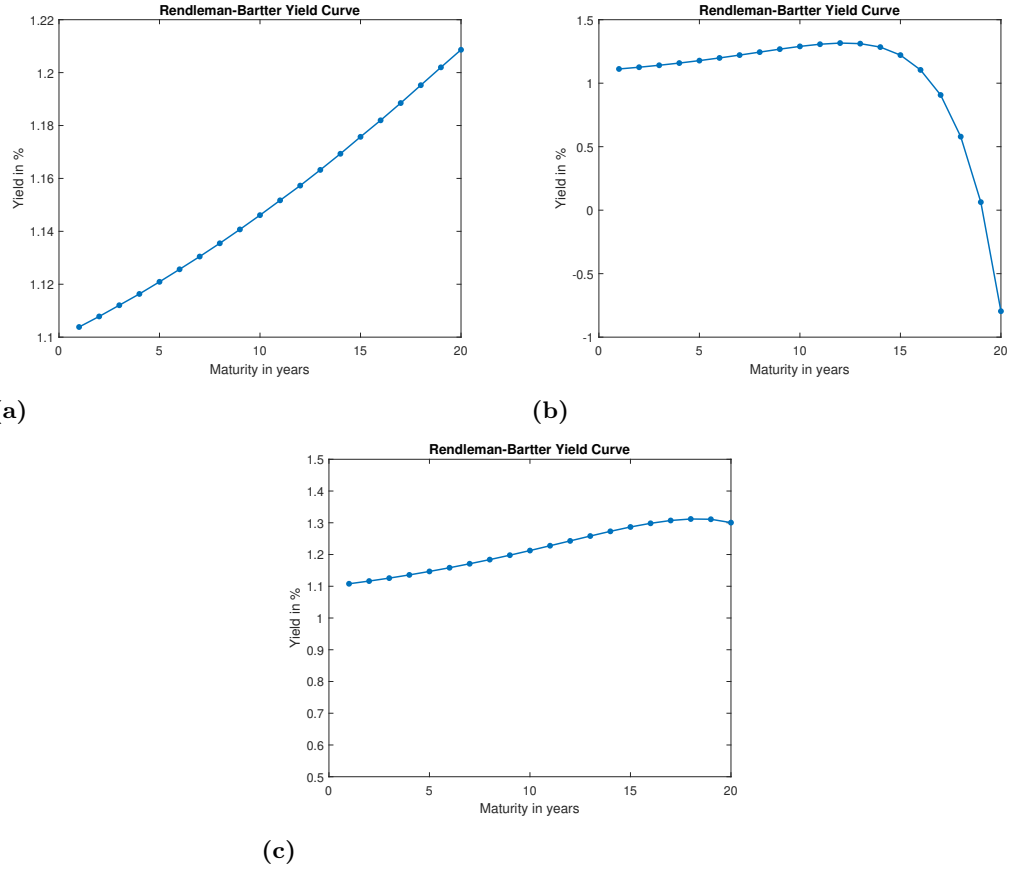

Figure 5.6: Yield curves in the Rendleman-Bartter model for parameter values where the interest rate is not mean-reverting. It can be seen that the yield to maturity does not flatten out for large maturities, like it does when the interest rate is mean-reverting.

6

Summary and Discussion

In summary, we have recreated each of the four main shapes that the yield curve commonly takes – normal, steep, inverted, and flat - for coupon bond yield curves in the four two-factor interest rate models that we have investigated. When fitting an interest rate model to real-world data, it is relevant to know that the model can recreate the qualitative behaviour of the yield curve, so this is a useful result.

To recreate the different yield curve shapes numerically, we have looked at the relationship between the initial value of the interest rate and the value that its mean reverts to for large times. In all models, a normal yield curve could be reproduced when the initial value of the interest rate was significantly smaller than the mean-reversion value. Similarly, an inverted yield curve could be reproduced when the initial value was significantly larger than the mean-reversion value, and a flat yield curve when the two values were roughly equal. To reproduce a steep yield curve, similarly to for a normal yield curve, we chose an initial value smaller than the mean-reversion value, but with a somewhat larger difference between the two values. We also choose a matrix of coefficients Λ that had smaller eigenvalues.

Recreating yield curve shapes by looking at the relationship between the initial value of the interest rate and its mean-reversion value is in line with the expectations hypothesis for explaining yield curve shapes. Recall that the hypothesis states that the yields for longer term bonds will be higher than the yields of shorter term bonds – as they are in a normal yield curve – if investors expect interest rates to rise in the future. The mean-reversion value of the interest rate can be seen as the value that the interest rate is expected to be at very far into the future, and thus if this value is larger than the initial – or present – value of the interest rate, we can say that this is equivalent to an expectation that the interest rate will rise. Similarly, the yields for shorter term bonds will be higher than the yields of longer term bonds – as they are in an inverted yield curve – when investors expect interest rates to fall in the future. This expectation is replicated by the initial value of the interest rate being chosen as larger than the mean-reversion value.

Choosing the initial value to be a lot smaller than the mean-reversion value to recreate a steep yield curve imitates the belief that interest rates will rise a lot in the future, producing a steeper slope. Choosing the eigenvalues of the matrix of coefficients Λ smaller reduces the rate of mean-reversion of the interest rate and produces a yield curve which does not flatten out as much for larger maturities, but there is not necessarily a real-world market motivation for this choice.

It seems that with increasing maturity, the yield to maturity converges to a value close to the mean-reversion value of the interest rate. With all parameter values the same, the yield to maturity seems to converge to different values in the different two-factor interest rate models that we have investigated. This indicates that the yield does not converge exactly to the mean-reversion value of the interest rate, since when all parameter values are the same, the mean-reversion value is the same for all models. It might be possible to analytically find the interest rate model-dependent value that the yield to maturity converges to for

large maturities, and to prove that it does in fact converge – similarly to how we showed that the interest rate is mean-reverting – but this has not been studied. It is not a straightforward problem, since getting the yield to maturity for even one coupon bond with a specific maturity involves solving an algebraic equation which depends on the coupons that the bond pays, as well as the initial price of the coupon bond, which according to the risk-neutral pricing formula depends on the expectation of a functional of the whole interest rate path.

We have also investigated the non-mean reverting version of the two-factor Rendleman-Bartter model, and found that the yield to maturity does not seem to converge to a constant value for large maturities, as it does when the interest rate is modelled by a mean-reverting process.

We have also noted that negative yields for low maturities can be recreated in the two-factor Vasicek, mixed, and Rendleman-Bartter models. In the CIR model, negative yields can only be produced if the coefficients that determine the relationship between the (strictly positive) model factors and the interest rate are chosen so that the interest rate becomes negative. When the interest rate remains positive for all times, as was originally the intention of the CIR model, it is seemingly not possible to recreate negative yields. When the CIR model was first introduced, it was thought to be a benefit that it never produced negative interest rates, but since in recent years some central banks have introduced negative interest rates, this is no longer necessarily true[12]. Furthermore, negative yields might have at one point been uncommon, but recently the yields for short maturity coupon bonds offered by the Swedish National Debt Office have been negative[1], so using a model that can recreate this could be a benefit.

We have also seen that allowing for nonzero constant correlation between the two Brownian motions in the two-factor interest rate models that we have investigated, does not seem to affect the yield curve or the zero coupon bond prices produced from the model, other than in the case of the two-factor Vasicek model. We note that this does not imply that the interest rate paths themselves are unaffected by allowing for correlation. However, it could be said that when working with two-factor affine yield models to price zero coupon bonds and produce yield curves, it might be enough to consider the case of zero correlation, where the quicker method of pricing zero coupon bonds by solving a system of coupled ordinary differential equations can be employed. We note also that for the two-factor Vasicek model, the ODE approach can be employed even for nonzero correlation.

Even though allowing for correlation between the two Brownian motions in the two-factor interest rate models studied here has been found to have no effect on the zero coupon bond prices in the models, it may still have an effect in other applications, financial or otherwise.

We present one further open problem. The problem of the factors $X_1(t)$ and $X_2(t)$ remaining strictly positive at all times in the two-factor CIR model, and the stochastic differential equations thus having a unique strong solution, has not been widely studied. A result applicable to a two-dimensional CIR process with independent Brownian motions can be found in [7], but no result exists for the case where the Brownian motions are correlated. It would thus be interesting to investigate how allowing for correlation between the Brownian motions that drive a two-dimensional CIR process affects the conditions for existence and uniqueness of the solution.

On the topic of numeric simulations, it could also be interesting to investigate whether a discretisation scheme like the one suggested in [14] could in fact be used in combination with a multi-level Monte-Carlo estimator.

Bibliography

[1] Swedish National Debt Office (Riksgälden). *Auction Results*. https://www.riksgalden.se/en/statistics/statistics-regarding-government-securities/auction-results/. Accessed: 2021-01-29.

[2] Abdel Berkaoui, Mireille Bossy, and Awa Diop. "Euler scheme for SDEs with non-Lipschitz diffusion coefficient: strong convergence". In: *ESAIM: Probability and Statistics* 12 (2008), pp. 1–11.

[3] Bloomberg.com. *United States Rates and Bonds*. https://www.bloomberg.com/markets/rates-bonds/government-bonds/us. Accessed: 2021-01-29.

[4] William E Boyce and Richard C DiPrima. *Elementary Differential Equations and Boundary Value Problems, Tenth Edition*. John Wiley & Sons, 2013.

[5] Simone Calogero. *Stochastic Calculus, Financial Derivatives and PDE's (Lecture notes)*. University of Gothenburg, 2020.

[6] Moorad Choudhry. *Analysing and interpreting the yield curve*. John Wiley & Sons, 2019.

[7] Darrell Duffie and Rui Kan. "A yield-factor model of interest rates". In: *Mathematical finance* 6.4 (1996), pp. 379–406.

[8] Emmanuel Gobet. *Monte-Carlo methods and stochastic processes: from linear to non-linear*. Chapman and Hall/CRC, 2016.

[9] Desmond J Higham. "An algorithmic introduction to numerical simulation of stochastic differential equations". In: *SIAM review* 43.3 (2001), pp. 525–546.

[10] Desmond J Higham. "An introduction to multilevel Monte Carlo for option valuation". In: *International Journal of Computer Mathematics* 92.12 (2015), pp. 2347–2360.

[11] John C. Hull. *Options, Futures, and Other Derivatives (Ninth Edition)*. Pearson Education Limited, 2018.

[12] Will Kenton Investopedia.com. *Cox-Ingersoll-Ross Model*. https://www.investopedia.com/terms/c/cox-ingersoll-ross-model.asp. Accessed: 2021-03-20.

[13] Fima C Klebaner. *Introduction to stochastic calculus with applications*. Imperial College Press, 2012.

[14] Chantal Labbé, Bruno Rémillard, and Jean-François Renaud. *A simple discretization scheme for nonnegative diffusion processes, with applications to option pricing*. 2010. arXiv: 1011.3247 [q-fin.CP].

[15] David Poole. *Linear algebra: A modern introduction*. Nelson Education, 2014.

[16] Steven E Shreve. *Stochastic calculus for finance II: Continuous-time models*. Vol. 11. Springer Science & Business Media, 2004.

[17] Investopedia.com Troy Segal. *The Predictive Powers of the Bond Yield Curve*. https://www.investopedia.com/articles/economics/08/yield-curve.asp. Accessed: 2021-03-20.

A

Sample Code

A.1 Vasicek Multi-Level Monte-Carlo Code

Sample code demonstrating the implementation of the multi level Monte-Carlo algorithm for the two-factor Vasicek model.

```
%% parameters
numPaths = 2^17; % number of interest rate paths
N = 8*2^10; % number of points for ZCB
initialValue = 0.02;
x0 = initialValue*ones(2*numPaths, 1); % initial condition
numPoints = 20; % number of points in yield curve
numLevels = 8; % number of levels of MLMC scheme

% SDE system parameters
a = [0.01 0.01]';
b = [1 -0.5; -0.5 1];
sigma = [0.1 0; 0 0.1];
correlation = -0.7;

% interest rate parameters:
% r = d1 + d2*X1 + d3*X2
d = [0.01 1/2 1/2];

%% calculating ZCB prices

maturities = (1:1:numPoints);

% calculating and storing values of zcbs
zcbPrices = zeros(1,numPoints);
zcbConf = zeros(1,numPoints);


for i = 1:numPoints
    i
    tic
    maturity = maturities(i);
    zcb = calculateZcbPriceVasicekMLMC(numLevels, maturity, numPaths, N, ...
        x0, a, b, sigma, d, correlation);
    zcbPrices(i) = zcb;
    toc
end

%% calculating coupon bond prices + yield curve

% coupon bond parameters
coupons = usTreasuryCoupons(numPoints);
couponFreq = 1;
firstCouponDate = 1;

```

```
yields = zeros(1, numPoints);

% coupon bond w maturity 1 year (no coupons)
couponBondPrice = zcbPrices(1);
yields(1) = -log(couponBondPrice);

% prices of all other coupon bonds
couponBondPrices = cumsum(zcbPrices)*diag(coupons);
couponBondPrices = couponBondPrices + zcbPrices;

for i = 2:numPoints
    maturity = maturities(i);
    coupon = coupons(i);
    initialPrice = couponBondPrices(i);
    yields(i) = calculateYield(initialPrice, coupon, couponFreq, ...
        firstCouponDate, maturity);
end

% plotting yield curve
figure
plot(maturities, 100*yields, 'LineWidth', 1.2,'Marker', '.', 'MarkerSize', 12)
title('Vasicek yield Curve')
ylabel('Yield in %')
xlabel('Maturity in years')

%% comparing ZCB prices with ODE method

zcbPricesOde = zeros(1,numPoints);

for i = 1:numPoints
    maturity = maturities(i);
    zcbPricesOde(i) = calculateZcbPriceVasicekOde45(maturity, initialValue, ...
        a, b, sigma, d, correlation);
end

% plotting zcb prices from monte carlo and ode methods for comparison
figure
plot(maturities, zcbPrices, 'LineStyle','none', 'Marker', '.', ...
    'MarkerSize', 12, 'Color', '#A2142F')
hold on
plot(maturities, zcbPricesOde, 'o', 'LineWidth', 1.5, 'Color','#4DBEEE')
hold off
title('Vasicek ZCB price comparison')
ylabel('ZCB price')
xlabel('Maturity in years')
legend('Monte Carlo price', 'ODE price','Location', 'best')
```

A.1.1 Functions

```
% function calculating the price of a zero coupon bond in the Vasicek model
% using multi level Monte-Carlo simulation

function zcbPrice = calculateZcbPriceVasicekMLMC(numLevels, maturity, ...
    finalNumPaths, finalNumPoints, x0, a, b, sigma, d, correlation)

% calculating correlation matrix
corrMatrix = [1 0; correlation sqrt(1 - correlation^2)];
weightedCorrMatrix = sigma * corrMatrix;

numPaths = finalNumPaths; %initial number of MC paths
numPoints = finalNumPoints/(2^numLevels); %initial number of points for ...
    Euler scheme

% zeroth level (regular MC estimation)
```

```
14  [zcbPrice,¬] = calculateZcbPrice(maturity, numPaths, numPoints, x0, a, b, ...
        sigma, d, correlation);
15
16  % main MLMC
17
18  for iLevel = 1:numLevels
19      numPaths = numPaths/4;
20      numPoints = numPoints*2;
21
22      x0 = x0(1:2*numPaths);
23      zcbPrice = zcbPrice + calculateMonteCarloLevelEstimate(maturity, ...
            numPaths, numPoints, x0, a, b, weightedCorrMatrix, d);
24  end
25
26
27  end
```

```
1   % function calculating the price of a zero coupon bond in the Vasicek model
2   % using regular Monte-Carlo simulation
3
4   function [zcbPrice, conf95] = calculateZcbPrice(maturity, numPaths, ...
        numPoints, x0, a, b, sigma, d, correlation)
5
6   dt = maturity/numPoints;
7   corrMatrix = [1 0; correlation sqrt(1 - correlation^2)];
8   weightedCorrMatrix = sigma * corrMatrix;
9
10
11  brownianPaths = generateBrownianPaths(dt, 2*numPaths, numPoints);
12  xPaths = zeros(2*numPaths, numPoints);
13
14
15  dB = brownianPaths(:,1);
16  xPaths(:,1) = eulerStep(x0, dt, dB, a, b, weightedCorrMatrix);
17  xTmp = xPaths(:,1);
18
19  for i = 2:numPoints
20
21      dB = brownianPaths(:,i) - brownianPaths(:,i-1);
22      xPaths(:,i) = eulerStep(xTmp, dt, dB, a, b, weightedCorrMatrix);
23      xTmp = xPaths(:,i);
24
25  end
26
27  % calculating price at time zero of zcb using risk-neutral pricing formula
28  interestRate = calculateInterestRate(xPaths, d);
29  interestRateIntegral = sum(interestRate, 2) * dt; % right Riemann sum to ...
        approximate integral
30  zcbValues = exp(-interestRateIntegral);
31  zcbPrice = mean(zcbValues);
32  conf95 = 1.96*std(zcbValues)/sqrt(numPaths);
33  end
```

```
1   % function that calculates the yield to maturity of coupon bonds. The
2   % coupons are assumed to all be equal, and the maturity and coupon dates
3   % must be integers (whole years)
4
5   function [yield] = calculateYield(initialPrice, coupon, couponFreq, ...
        firstCouponDate, maturity)
6
7   coefficients = zeros(maturity + 1, 1);
8
9   coefficients(1) = 1+coupon; %highest order term
10
```

```
date = firstCouponDate + couponFreq;

while date ≤ maturity

    coefficients(date) = coupon;
    date = date + couponFreq;

end

coefficients(end) = - initialPrice;

yieldRoots = roots(coefficients);
yieldRoots = yieldRoots(imag(yieldRoots)==0);
yieldRoots = yieldRoots(yieldRoots>0);

yield = -log(yieldRoots);


end
```

```
% function that calculates the price of a zcb in the Vasicek model by
% using the ODE approach

function [zcbPrice] = calculateZcbPriceVasicekOde45(maturity, x0, a, b, ...
    sigma, d, rho)

tspan = [0 maturity];
y0 = [0 0 0];
[t,y] = ode45(@(t,y) odefunVasicek(t,y,a,b,sigma,d,rho), tspan, y0);

finalA = y(end,3);
finalC = y(end,1:2);

initialX = x0*ones(1,2)';

zcbPrice = exp(-finalC*initialX - finalA);
```

```
function dydt = odefunVasicek(t,y,a,b,sigma,d,rho)
dydt = zeros(3,1);
dydt(1) = d(2) - b(1,1)*y(1) - b(2,1)*y(2);
dydt(2) = d(3) - b(1,2)*y(1) - b(2,2)*y(2);
dydt(3) = d(1) + a(1)*y(1) + a(2)*y(2) - 0.5*sigma(1,1)^2*y(1)^2 - ...
    0.5*sigma(2,2)^2*y(2)^2 - rho*sigma(1,1)*sigma(2,2)*y(1)*y(2);
end
```

```
% function calculating one of the terms in the sum that makes up the multi
% level Monte-Carlo estimator

function meanDifference = calculateMonteCarloLevelEstimate(maturity, ...
    numPaths, numPoints, x0, a, b, sigma, d)

timeStep = maturity/numPoints;

% generating brownian motion paths (the same path at two levels of
% coarseness)
finerBrownianPaths = generateBrownianPaths(timeStep, 2*numPaths, numPoints);
coarserBrownianPaths = finerBrownianPaths(:,1:2:end);

% calculating paths of the 2d stochastic process X using the two different
% versions of Brownian motion paths

% Using the finer Brownian paths
```

```
dt1 = timeStep;
xPathsFiner = zeros(2*numPaths, numPoints);
dB = finerBrownianPaths(:,1);
xPathsFiner(:,1) = eulerStep(x0, dt1, dB, a, b, sigma);
xTmp = xPathsFiner(:,1);

for i = 2:numPoints

    dB = finerBrownianPaths(:,i) - finerBrownianPaths(:,i-1);
    xPathsFiner(:,i) = eulerStep(xTmp, dt1, dB, a, b, sigma);
    xTmp = xPathsFiner(:,i);

end

% Using the coarser Brownian paths
dt2 = timeStep*2;
xPathsCoarser = zeros(2*numPaths, numPoints/2);
dB = coarserBrownianPaths(:,1);
xPathsCoarser(:,1) = eulerStep(x0, dt2, dB, a, b, sigma);
xTmp = xPathsCoarser(:,1);

for i = 2:numPoints/2

    dB = coarserBrownianPaths(:,i) - coarserBrownianPaths(:,i-1);
    xPathsCoarser(:,i) = eulerStep(xTmp, dt2, dB, a, b, sigma);
    xTmp = xPathsCoarser(:,i);

end

% calculating interest rate paths
finerInterestRate = calculateInterestRate(xPathsFiner, d);
coarserInterestRate = calculateInterestRate(xPathsCoarser, d);

% calculating integrals
finerInterestRateIntegral = sum(finerInterestRate, 2) * dt1; % RIGHT ...
    Riemann sum to approximate integral
coarserInterestRateIntegral = sum(coarserInterestRate, 2) * dt2;

finerZcbValues = exp(-finerInterestRateIntegral);
coarserZcbValues = exp(-coarserInterestRateIntegral);

% calculating the mean difference between results found with coarser and
% finer paths
difference = finerZcbValues - coarserZcbValues;
meanDifference = mean(difference);
end
```

```
% function that generates the next Euler-Maruyama step in the two-factor
% Vasicek model

function [nextXPoints] = eulerStep(prevXPoints, dt, dB, a, b, sigma)

numPaths = length(prevXPoints);
nextXPoints = zeros(numPaths, 1);

for i = 1:2:numPaths-1
    xTmp = prevXPoints(i:i+1,:);
    dBTmp = dB(i:i+1, :);
    nextXPoints(i:i+1, :) = xTmp + (a - b*xTmp) * dt + sigma * dBTmp;
end

end
```

```
% this function generates numPaths (independent) Brownian motion paths, ...
    each consisting
% of numPoints points. The timeStep is constant. The initial value B_0 = 0
% is NOT included. Each row is one path.

function [brownianPaths] = generateBrownianPaths(timeStep, numPaths, numPoints)

brownianPaths = zeros(numPaths, numPoints);

brownianPaths(:,1) = sqrt(timeStep) * randn(numPaths,1);

for iStep = 2:numPoints
    brownianPaths(:,iStep) = brownianPaths(:,iStep - 1) + sqrt(timeStep) * ...
        randn(numPaths,1);
end

end
```

```
% function that interpolates coupon values for coupon bonds inspired by
% bonds offered by the US Treasury

function coupons = usTreasuryCoupons(numPoints)

x = [2 5 10 30];
v = [0.13 0.38 0.88 1.63];
xq = (1:1:numPoints);

coupons = 0.01*interp1(x,v,xq);
end
```

```
function interestRate = calculateInterestRate(xPaths, d)

d0 = d(1);
d1 = d(2);
d2 = d(3);

numPaths = size(xPaths, 1)/2;
numPoints = size(xPaths, 2);

interestRate = zeros(numPaths, numPoints);

for i = 1:numPaths

    interestRate(i,:) = d0 + d1 * xPaths(2*i-1,:) + d2 * xPaths(2*i,:);

end

end
```

A.2 CIR Model Code

Sample code demonstrating the implementation of the weak scheme from [14] for the two factor CIR model.

```
%% parameters
numPaths = 2^15; % number of interest rate paths
N = 100; % number of points for ZCB
initialValue = 0.01;
x0 = initialValue*ones(2*numPaths, 1); % initial condition
numPoints = 20; % number of points in yield curve
```

```
7
8  % SDE system parameters
9  a = [0.5 0.5]';
10 b = [2 -0.5; -1 1];
11 sigma = [1 0; 0 1];
12 bernoulliMean = 1;
13 correlation = -0.8;
14
15 % interest rate parameters:
16 % r = d1 + d2*X1 + d3*X2
17 d = [0.01 1/2 1/2];
18
19
20 %% calculating ZCB prices
21 maturities = (1:1:numPoints);
22
23 % calculating and storing values of zcbs
24 zcbPrices = zeros(1,numPoints);
25 zcbConf = zeros(1,numPoints);
26
27
28 for i = 1:numPoints
29     maturity = maturities(i);
30     [zcb, conf] = calculateZcbPriceCIRBernoulli(maturity, numPaths, N, x0, ...
           a, b, sigma, d, bernoulliMean, correlation);
31     zcbPrices(i) = zcb;
32     zcbConf(i) = conf;
33 end
34
35 %% calculating coupon bond prices + yield curve
36
37 % coupon bond parameters
38 coupons = usTreasuryCoupons(numPoints);
39 couponFreq = 1;
40 firstCouponDate = 1;
41
42 yields = zeros(1, numPoints);
43
44 % coupon bond w maturity 1 year (no coupons)
45 couponBondPrice = zcbPrices(1);
46 yields(1) = -log(couponBondPrice);
47
48 % prices of all other coupon bonds
49 couponBondPrices = cumsum(zcbPrices)*diag(coupons);
50 couponBondPrices = couponBondPrices + zcbPrices;
51
52 for i = 2:numPoints
53     maturity = maturities(i);
54     coupon = coupons(i);
55     initialPrice = couponBondPrices(i);
56     yields(i) = calculateYield(initialPrice, coupon, couponFreq, ...
           firstCouponDate, maturity);
57 end
58
59 % plotting yield curve
60 figure
61 plot(maturities, 100*yields, 'LineWidth', 1.2,'Marker', '.', 'MarkerSize', 12)
62 title('CIR yield Curve')
63 ylabel('Yield in %')
64 xlabel('Maturity in years')
65
66 %% comparing ZCB prices with ODE method
67
68 zcbPricesOde = zeros(1,numPoints);
69
70 for i = 1:numPoints
71     maturity = maturities(i);
```

```
72      zcbPricesOde(i) = calculateZcbPriceCirOde45(maturity, initialValue, a, ...
            b, sigma, d);
73  end
74
75  % plotting zcb price comparison
76  figure
77  plot(maturities, zcbPrices, 'LineStyle','none', 'Marker', '.', ...
        'MarkerSize', 12, 'Color', '#A2142F')
78  hold on
79  plot(maturities, zcbPricesOde, 'o', 'LineWidth', 1.5, 'Color','#4DBEEE')
80  hold off
81  title('CIR ZCB price comparison')
82  ylabel('ZCB price')
83  xlabel('Maturity in years')
84  legend('Monte Carlo price', 'ODE price','Location', 'best')
```

A.2.1 Functions

```
1   function [zcbPrice, conf95] = calculateZcbPriceCIRBernoulli(maturity, ...
        numPaths, numPoints, x0, a, b, sigma, d, bernoulliMean, correlation)
2
3   dt = maturity/numPoints;
4
5   xPaths = zeros(2*numPaths, numPoints);
6
7   xPaths(:,1) = eulerStepCIRBernoulli(x0, dt, a, b, sigma, bernoulliMean, ...
        correlation);
8   xTmp = xPaths(:,1);
9
10  for i = 2:numPoints
11
12      xPaths(:,i) = eulerStepCIRBernoulli(xTmp, dt, a, b, sigma, ...
            bernoulliMean, correlation);
13      xTmp = xPaths(:,i);
14
15  end
16
17  % calculating price at time zero of zcb using risk-neutral pricing formula
18  interestRate = calculateInterestRate(xPaths, d);
19  interestRateIntegral = sum(interestRate, 2) * dt; % right Riemann sum to ...
        approximate integral
20  zcbValues = exp(-interestRateIntegral);
21  zcbPrice = mean(zcbValues);
22  conf95 = 1.96*std(zcbValues)/sqrt(numPaths);
23
24  end
```

```
1   function [nextXPoints] = eulerStepCIRBernoulli(prevXPoints, dt, a, b, ...
        sigma, bernoulliMean, correlation)
2
3   numPaths = length(prevXPoints);
4   nextXPoints = zeros(numPaths, 1);
5
6   for i = 1:2:numPaths-1
7       xTmp = prevXPoints(i:i+1,:);
8       randStep = generateBernoulliVector(correlation, bernoulliMean);
9       nextX = xTmp + (a - b*xTmp) * dt + sigmaCIR(xTmp, sigma) * randStep * ...
            sqrt(dt);
10      nextXPoints(i:i+1, :) = nextX;
11  end
12
13  end
```

```
% function that generates a Bernoulli-type random 2d vector with specified
% correlation between the components

function [randomVector] = generateBernoulliVector(correlation, mean)

corrMatrix = [1 0; correlation sqrt(1-correlation^2)];

bernoulliParam = mean^2/(1 + mean^2);
unif = rand(2,1);
bernoulliVector = zeros(2,1);

for i = 1:2
    if unif(i) < bernoulliParam
        bernoulliVector(i) = 1;
    end
end

scaleFactor = (1 + mean^2)/mean;

randomVector = scaleFactor*corrMatrix*bernoulliVector;
meanVector = mean*[1 correlation+sqrt(1-correlation^2)]';

randomVector = randomVector - meanVector;

end
```

```
function [zcbPrice] = calculateZcbPriceCirOde45(maturity, x0, a, b, sigma, d)

tspan = [0 maturity];
y0 = [0 0 0];
[t,y] = ode45(@(t,y) odefunCIR(t,y,a,b,sigma,d), tspan, y0);

finalA = y(end,3);
finalC = y(end,1:2);

initialX = x0*ones(1,2)';

zcbPrice = exp(-finalC*initialX - finalA);

end
```

```
function dydt = odefunCIR(t,y,a,b,sigma,d)
dydt = zeros(3,1);
dydt(1) = d(2) - b(1,1)*y(1) - b(2,1)*y(2) - 0.5*sigma(1,1)^2*y(1)^2;
dydt(2) = d(3) - b(1,2)*y(1) - b(2,2)*y(2) - 0.5*sigma(2,2)^2*y(2)^2;
dydt(3) = d(1) + a(1)*y(1) + a(2)*y(2);
end
```

B

Convergence Plots

We briefly present some weak convergence plots for the estimates of zero coupon bond prices in the different models. The weak error is here defined as the absolute value of the difference between the theoretical value of the zero coupon bond according to the risk-neutral pricing formula, and the approximated value from the numerical methods, where all our numerical methods include some form of Euler-Maruyama scheme and some form of Monte-Carlo estimator. This is a weak error since it estimates the difference between the theoretical value of the expectation in the risk-neutral pricing formula, and the approximated value of that expectation obtained using numerical methods. In other words, the error is of the form

$$|\mathbb{E}[Y] - \overline{Y}|. \tag{B.1}$$

Since the exact, theoretical ZCB price is not known in any of the models considered – other than the Vasicek model – a numerical solution computed on a finer grid is used in place of $\mathbb{E}[Y]$ to get an approximate weak error. In figure B.1, the weak error is plotted against the timestep h of the Euler-Maruyama-type discretisation schemes.

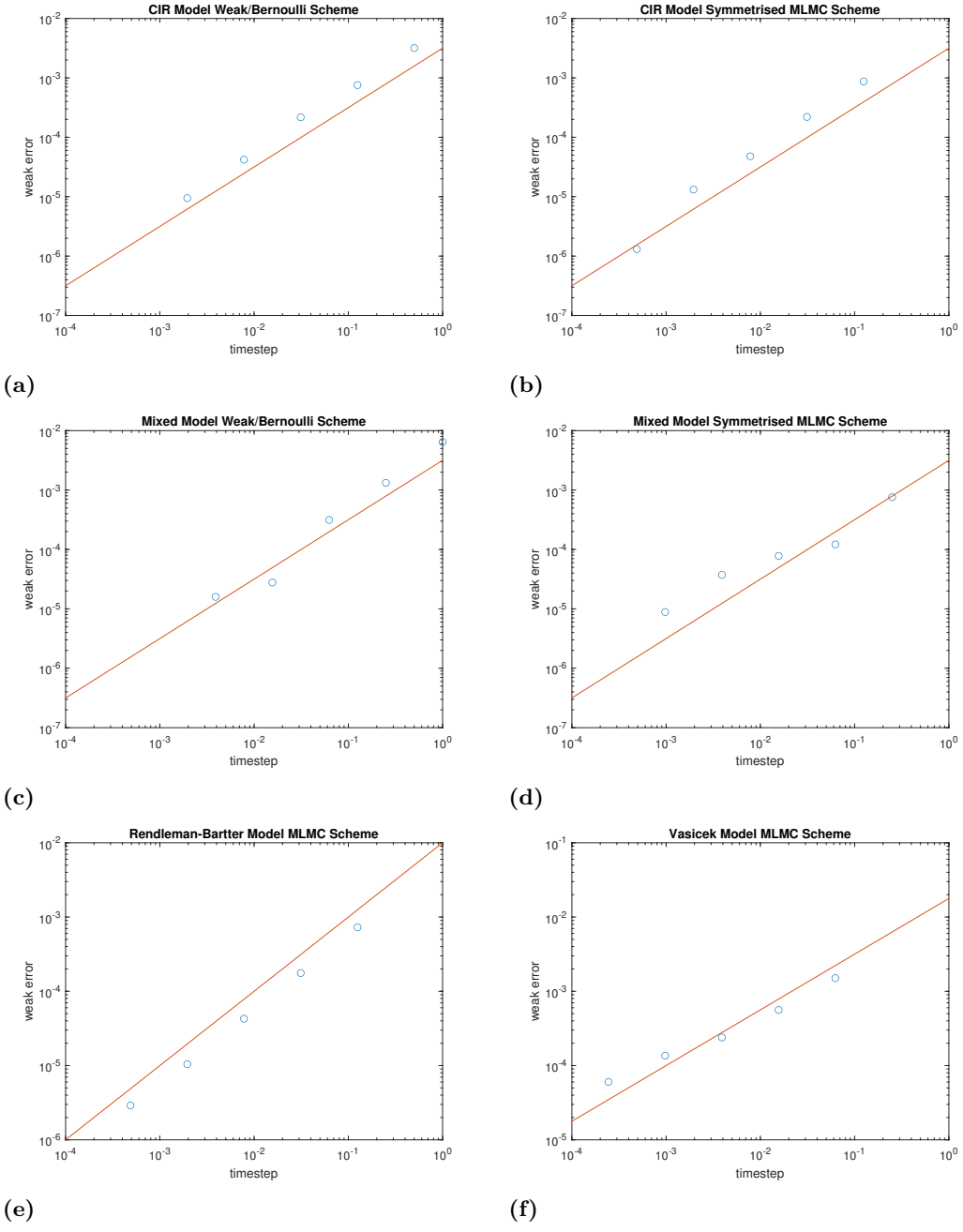

Figure B.1: Weak convergence plots. The blue dots indicate the weak error at different time steps h, and the red line in each plot is a reference straight line. All plots are plotted on a logarithmic scale on both axes.